Computers and Concrete, *Vol. 22, No. 4 (2018) 419-437*
DOI: https://doi.org/10.12989/cac.2018.22.4.419

Predicting the compressive strength of self-compacting concrete containing fly ash using a hybrid artificial intelligence method

Emadaldin M. Golafshani* and Gholamreza Pazouki[a]

Department of Civil Engineering, Architecture and Art, Science and Research Branch, Islamic Azad University, Tehran, Iran

(Received April 29, 2018, Revised September 24, 2018, Accepted October 11, 2018)

Abstract. The compressive strength of self-compacting concrete (SCC) containing fly ash (FA) is highly related to its constituents. The principal purpose of this paper is to investigate the efficiency of hybrid fuzzy radial basis function neural network with biogeography-based optimization (FRBFNN-BBO) for predicting the compressive strength of SCC containing FA based on its mix design i.e., cement, fly ash, water, fine aggregate, coarse aggregate, superplasticizer, and age. In this regard, biogeography-based optimization (BBO) is applied for the optimal design of fuzzy radial basis function neural network (FRBFNN) and the proposed model, implemented in a MATLAB environment, is constructed, trained and tested using 338 available sets of data obtained from 24 different published literature sources. Moreover, the artificial neural network and three types of radial basis function neural network models are applied to compare the efficiency of the proposed model. The statistical analysis results strongly showed that the proposed FRBFNN-BBO model has good performance in desirable accuracy for predicting the compressive strength of SCC with fly ash.

Keywords: self-compacting concrete; fly ash; compressive strength; fuzzy radial basis function neural network; biogeography-based optimization

1. Introduction

Self-compacting concrete (SCC) is relatively an emerging technology which has brought a new insight into the construction industry. It was first developed in the late 1980s in Japan to be used in the construction of skyscrapers and was adopted in Europe, North America and the rest of the world (Ozawa *et al.* 1990, Sonebi 2004). This type of high performance concrete is a highly workable concrete which can easily flow under its own weight, pass through congested reinforcing bars, fill small interstices of formwork with minimal compaction and without apparent segregation and blocking (Golafshani *et al.* 2014, Liu 2010, Melo and Carneiro 2010, Persson 2001, Phan *et al.* 2006, Siddique 2011, Sonebi 2004, Zhu *et al.* 2001). Its introduction represents a major technological advance which led to a better quality of concrete, enhancement towards the productivity and automation of precast products and substantial improvement of working environment on site (Ghezal and Khayat 2002, Sonebi and Cevik 2009a, Zhu and Bartos 2003).

The mix designs of SCC and normal concrete are different. Chemical additives such as high-range water reducing and/or viscosity modified admixtures and also powder materials are used in SCC production (Bingöl and Tohumcu 2013, Golafshani and Ashour 2016b, Mohamed 2011, Sonebi 2004). Three essential properties of SCC are filling ability, passing ability and segregation resistance (Bingöl and Tohumcu 2013, El-Dieb and Reda Taha 2012, Liu 2010). In order to avoid segregation in SCC, the amount of coarse aggregate should be limited which leads to higher cement consumption in its mix design. Moreover, the cost of SCC production increases, if adding more cement is the only solution (Liu 2010). One solution to decrease the cost of SCC production is to use the mineral admixtures such as silica fume, fly ash (FA), blast furnace slag, rice husk ash, etc. which are finely grained materials added to SCC during mixture procedure (Şahmaran *et al.* 2006, Uysal and Sumer 2011). The cost of SCC production reduces when the mineral admixtures replace part of the cement in SCC mix design, especially in the case of waste or industrial by-product admixtures. FA is a fine grained residue of coal combustion in coal-fired power plant which is commonly used to produce concrete for many decades. The usage of this mineral material in SCC, as a by-product of industrial process, can assist the challenges of sustainable construction in the 21st century (Shaikh and Supit 2014, 2015). The utilization of FA in construction industry has become a commercial product with an achievement of approximately 55% during 2010-2012 (Utilisation 2008). Application of FA in SCC can improve the workability and cohesiveness, increase the long-term compressive strength, reduce the segregation, lower the cost by replacing relatively costlier cement, lower the heat of hydration, lower the permeability, lower the shrinkage and creep of SCC (Patel *et al.* 2004).

The concrete compressive strength is one of the major parameters in design of reinforced concrete structures which mainly affected by the constituents of concrete. Predicting the concrete compressive strength is more

*Corresponding author, Assistant Professor
E-mail: Golafshani@srbiau.ac.ir
[a]MSc Student

http://www.techno-press.org/?journal=cac&subpage=8
ISSN: 1598-8198 (Print), 1598-818X (Online)

Table 1 Different AI methods applied for predicting the compressive strength of various types of concrete

Concrete type	Applied artificial intelligence methods in literature
Concrete containing mineral admixtures	ANN (Atici 2011, Bilim *et al.* 2009, Boğa *et al.* 2013, Khan 2012, Özcan *et al.* 2009, Pala *et al.* 2007, Saridemir 2009a, Sarıdemir *et al.* 2009, Topçu and Sarıdemir 2008, Valipour *et al.* 2013), FL (Özcan *et al.* 2009, Saridemir 2009b, Sarıdemir *et al.* 2009, Topçu and Sarıdemir 2008), GP (Boğa *et al.* 2013, Gilan *et al.* 2012, Sarıdemir 2014), Evolutionary ANN (Behnood and Golafshani 2018, Rebouh *et al.* 2017)
High-performance concrete	ANN (Khan 2012, Öztaş *et al.* 2006, Słoński 2010, Tayfur *et al.* 2014), FL (Tayfur *et al.* 2014), Genetic extension programming (Baykasoğlu *et al.* 2009, Castelli *et al.* 2013, Mousavi *et al.* 2012), least squares support vector regression (Pham *et al.* 2016), Time-weighted evolutionary fuzzy support vector machines inference model (Cheng *et al.* 2012), Enhanced artificial intelligence ensemble approach (Chou and Pham 2013), Genetic weighted pyramid operation tree (Cheng *et al.* 2014), Evolutionary ANN (Bui *et al.* 2018).
Self-compacting concretes	ANN (Ashteyat and Ismeik 2018, Saha *et al.* 2017, Siddique *et al.* 2011, Uysal and Tanyildizi 2012, 2011), GP (Ozbay *et al.* 2008, Sonebi and Cevik 2009a), ANFIS (Sonebi and Cevik 2009b), Particle swarm optimization algorithm and ANN (Mashhadban *et al.* 2016), least squares support vector regression (Aiyer *et al.* 2014).

complicated when the constituents of concrete change and one or more chemical or mineral admixtures are added to it. Several researchers have attempted to predict the compressive strength of different types of concrete using various artificial intelligence (AI) methods and have proved the high performance of these methods. Table 1 shows a comprehensive list of recent researches about application of AI methods in estimating the compressive strength of various types of concrete. As demonstrated in this Table, most researchers have applied well-known AI methods such as artificial neural network (ANN), fuzzy model (FL) and genetic programming (GP) for predicting the compressive strength of various types of concrete. Moreover, there are limited researches in predicting the compressive strength of various types of SCC using hybrid AI methods. Some applications of AI methods in calculating the compressive strength of SCC are mentioned in the following.

Ozbay *et al.* (2008) introduced GP as a quite reliable method for formulating the fresh and hardened properties of SCC. Sonebi and Cevik (2009a, b) showed the strong potential of GP and neuro-fuzzy methods to model and formulate the fresh and hardened properties of self-compacting concrete (SCC) containing pulverised fuel ash (PFA) based on their experimental work. Uysal and Tanyildizi (2011) offered that ANN can be an alternative approach to predict the core compressive strength of SCC mixtures with mineral additives. In addition, they (Uysal and Tanyildizi 2012) proposed an ANN model with reasonable error for predicting the compressive strength of SCC containing mineral additives and polypropylene (PP) fiber exposed to elevated temperature. Siddique *et al.* (2011) showed the proper predictions of ANN in modeling the compressive strength of SCC containing bottom ash. Mashhadban *et al.* (2016) introduced ANN as a flexible and accurate method in prediction of mechanical properties of fiber reinforced SCC properties. Aiyer *et al.* (2014) examined the capability of support vector machine (SVM) and least square SVM for determination of compressive strength of SCC and confirmed that the developed models can be effective tools for solving different problems in concrete. Ashteyat and Ismeik (2018) served the ANN model to predict the compressive strength of SCC under different temperatures and relative humidity conditions and achieved reliable results. Saha *et al.* (2017) employed ANN as a powerful tool in estimating the compressive strength of SCC.

The aim of this study is to predict the compressive strength of SCC containing FA as a function of important input parameters, namely, cement, fly ash, water, fine aggregate, coarse aggregate, superplasticizer and age. This is accomplished by using hybrid fuzzy radial basis function neural network with biogeography-based optimization (FRBFNN-BBO) as a novel hybrid AI method which is a mixture of fuzzy set theory, a strong type of neural network, called radial basis function neural network, and a powerful meta-heuristic optimization algorithm. The rest of this paper is structured as follows: In section 2 a comprehensive explanation about FRBFNN-BBO are given. Section 3 describes the model development of FRBFNN-BBO for predicting the compressive strength of SCC containing fly ash. The results of the compressive strength prediction methodology are presented and discussed in Section 4 and finally study conclusions are given in Section 5.

2. Architecture and learning of FRBFNN

In this section, different parts of FRBFNN-BBO are presented and finally the learning algorithm of FRBFNN-BBO is explained.

2.1 Fuzzy C-Means Clustering (FCM) method for information granulation

Generally speaking, information granules are intuitively appealing constructs, which play a fundamental role in human cognitive and decision-making activities (Pedrycz *et al.* 2015). They are formed as associated or linked collections of objects (in particular, data points) being absorbed together based on their similarities (Ivakhnenko 1971). Information granulation is supported by a series of procedures that are used to extract meaningful concepts from numeric data or other sources of experimental data. Clustering and fuzzy clustering are common methods when dealing with information granulation using numeric data (Roh *et al.* 2011, Sánchez *et al.* 2009). Fuzzy C-Means

(FCM) clustering algorithm (Peizhuang 1983) is one of the attractive methods of information granulation which explained briefly in the following.

Fuzzy clustering is a technical method in which each data point can belong to different clusters using fuzzy logic and provides effective tools for separating overlapping clusters. This algorithm is more suitable for the applications with continuous or overlapping profiles (Sandhir *et al.* 2012). Fuzzy *c*-means (FCM) algorithm are the most reputable and widely used fuzzy separation clustering techniques. It is a set-partitioning method based on Picard iteration through necessary conditions for optimizing a weighted sum of squared errors objective function (J_m). Let $c \geq 2$ be the number of clusters, $X = (X_1, \ldots, X_P) \subset R^n$ be a finite data set containing at least $c<P$ distinct points and R^{cP} denote the set of all real $c \times P$ matrices. A non-degenerate fuzzy *c*-partition of X is conveniently represented by a partition matrix $U=[u_{ki}] \subset R^{cP}$, the entries of which satisfy (Mitra and Basak 2001)

$$\mathrm{u_{ki}} \in [0,1], \qquad 1 \leq \mathrm{k} \leq \mathrm{c}, \quad 1 \leq \mathrm{i} \leq \mathrm{P} \tag{1}$$

$$\sum_{\mathrm{k}=1}^{\mathrm{c}} \mathrm{u_{ki}} = 1, \quad 1 \leq \mathrm{i} \leq \mathrm{P} \tag{2}$$

$$\sum_{\mathrm{i}=1}^{\mathrm{P}} \mathrm{u_{ki}} > 0, \quad 1 \leq \mathrm{k} \leq \mathrm{c} \tag{3}$$

The set of all matrices in R^{cP} satisfying Eqs. (1)-(3) is denoted by M_{fcP}. A matrix $U \in M_{fcP}$ can be used to describe the cluster structure of X by interpreting u_{ki} as the grade of membership of X_i in the *k*th cluster. Other useful information about cluster substructure can be achieved by identifying cluster centers $v=(v_1,\ldots, v_c)^T \in R^{cn}$, where $\mathrm{v_k}$ is the prototype for class k, $1 \leq k \leq c$, $v_k \in R_n$. 'Good' partitions U of X and representatives (v_k for class k) may be defined by considering minimization of the *c*-means objective function J_m: $(M_{fcP} \times R^{cn}) \rightarrow R$, defined by (Mitra and Basak 2001)

$$\mathrm{J_m(U,v)} = \sum_{\mathrm{i}=1}^{\mathrm{P}} \sum_{\mathrm{k}=1}^{\mathrm{c}} (\mathrm{u_{ki}})^{\mathrm{m}} \|\mathrm{X_i} - \mathrm{v_k}\|^2 \tag{4}$$

where $1 \leq m < \infty$ is the fuzzification coefficient and $\|.\|$ is any inner product induced norm on R^n. For $m>1$, Bezdek (Peizhuang 1983) gave the following necessary conditions for a minimizer (U^*,v^*) of $J_m(U,v)$ over $M_{fcP} \times R^{cn}$

$$\mathrm{v_k^*} = \frac{\sum_{\mathrm{i}=1}^{\mathrm{P}} (\mathrm{u_{ki}^*})^{\mathrm{m}} \mathrm{X_i}}{\sum_{\mathrm{i}=1}^{\mathrm{P}} (\mathrm{u_{ki}^*})^{\mathrm{m}}} \tag{5}$$

where

$$\mathrm{u_{ki}^*} = \left(\sum_{\mathrm{r}=1}^{\mathrm{c}} \left(\frac{\|\mathrm{X_i} - \mathrm{v_k^*}\|}{\|\mathrm{X_i} - \mathrm{v_r^*}\|} \right)^{2/(\mathrm{m}-1)} \right)^{-1} \tag{6}$$

2.2 Radial Basis Function Neural Network (RBFNN)

Generally, a RBFNN consists of three layers, namely the input, hidden and output layers. The structure of an *n* inputs and *m* outputs RBFNN is depicted in Fig. 1. The input layer receives data from the environment and transmits them to the hidden layer. A radial basis function is assigned to each neuron in the hidden layer. The inputs of hidden layer are the linear combinations of scalar weights and input vector. Therefore, the whole input vector transits to each neuron in the hidden layer. The incoming vectors are being mapped by the radial basis functions in each hidden node. In the output layer, the linear weighted sum of the activated values of the all hidden neurons is calculated as network output, which can be expressed as (Yang *et al.* 2013)

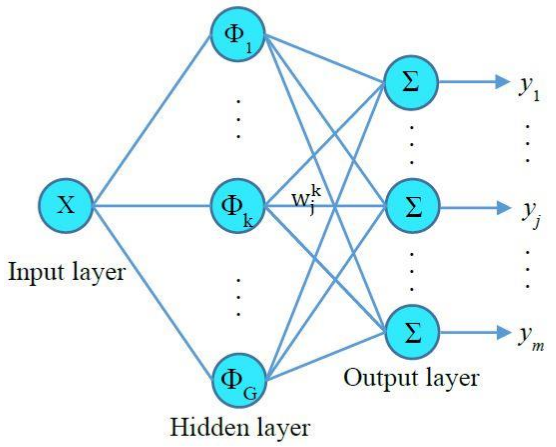

Fig. 1 The architecture of a RBFNN model

$$\mathrm{y_{ij}} = \sum_{\mathrm{k}=1}^{\mathrm{G}} \mathrm{w_j^k} \varnothing_{\mathrm{ik}}^{\mathrm{N}}(\mathrm{X_i}), \qquad \text{for j=1,...,m} \tag{7}$$

where $X_i = (x_{i1}, \ldots, x_{in})$ and $Y_i = (y_{i1}, \ldots, y_{ij} \ldots, y_{im})$ are the input and the corresponding output related to the *i*th pattern, respectively. $\varnothing_{ik}^N$ is the normal RBF value of the *k*th hidden node related to the *i*th pattern and w_j^k denotes the weight between the *k*th hidden node and *j*th output node. In addition, G is the total number of hidden nodes. The most frequently used RBF is the Gaussian function which can be formulated as follow

$$\varnothing_{\mathrm{ik}}(\mathrm{X_i}) = \exp\left(-\frac{\|\mathrm{X_i} - \mathrm{v_k}\|^2}{2\sigma_{\mathrm{k}}^2} \right), \quad \text{for } \mathrm{k} = 1, \ldots, \mathrm{G} \tag{8}$$

where $v_k = (v_{k1}, \ldots, v_{kn})$ and $\sigma_k = (\sigma_{k1}, \ldots, \sigma_{kn})$ are the center and spread width of the *k*th RBF in the hidden layer, respectively. The normalized RBF value in Eq. (7) can be derived as follow

$$\varnothing_{\mathrm{ik}}^{\mathrm{N}}(\mathrm{X_i}) = \frac{\varnothing_{\mathrm{ik}}(\mathrm{X_i})}{\sum_{\mathrm{k}=1}^{\mathrm{G}} \varnothing_{\mathrm{ik}}(\mathrm{X_i})} \tag{9}$$

In general, the RBFNN training can be divided into two phases:

(1) Determine the number of RBFs and their parameters, i.e., Gaussian center and spread width.

(2) Determine the output weight w_j^k by supervised learning method. Usually Least-Mean-Square (LMS) or Recursive Least-Square (RLS) are applied (Yang *et al.* 2013).

More information about RBFNN and training process can be found in (Yang *et al.* 2013).

2.3 Fuzzy radial basis function neural network

Specifying the number of hidden nodes, the values of

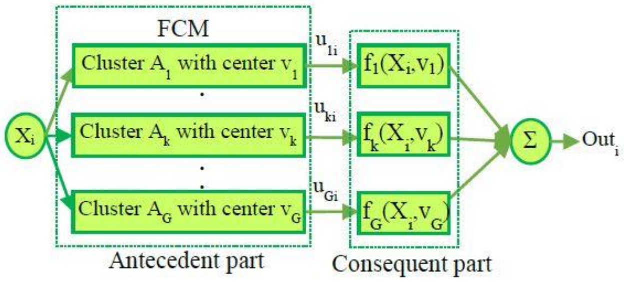

Fig. 2 The architecture of a FRBFNN model

centers and spreads of RBFs are very important part of RBFNN. In FRBFNN, RBFNN and fuzzy inference system (FIS) share some commonalities (Mantas and Puche 2008). As shown in Fig. 2, the number of RBFs is equal to the number of fuzzy "if-then" rules of FIS in the architecture of FRBFNN. Each RBF in FRBFNN is described by a membership function with a predetermined center in the antecedent part of the corresponding rule. In FRBFNN, FCM is used to calculate the centers of the antecedent parts of fuzzy rules and also determination of belonging values of the patterns to the clusters. The weight of link between the antecedent and consequence part of each fuzzy rule is the belonging value of a pattern to the corresponding cluster. For clarification purpose, consider a system with n input variables and one output and assume that $X = \{x_1, \ldots, x_i, \ldots, x_p\}$ is the all input patterns and $x_i = \{x_{i1}, \ldots, x_{ij}, \ldots, x_{in}\}$ is the ith input pattern.

The form of "if-then" rules can be expressed as follow

$$\begin{aligned} &\mathrm{R^k}\text{: if } \mathrm{X_i} \text{ is included in cluster } \mathrm{A_k} \text{ with center } \mathrm{v_k} \\ &\text{Then} \quad \mathrm{y_{ik}} = \mathrm{f_k}(\mathrm{X_i}, \mathrm{v_k}), \quad 1 \le \mathrm{k} \le \mathrm{G} \end{aligned} \tag{10}$$

where R^k is the kth fuzzy rule, G is the number of fuzzy rules (is equal to the number of clusters or RBFs), A_k is the kth membership function, $v_k = \{x_{k1}, \ldots, x_{kj}, \ldots, x_{kn}\}$ is the center of A_k, y_{ik} is the consequence value of the kth rule for X_i and f_k is a consequent polynomial in the kth fuzzy rule. Different forms of consequent polynomial are given in Table 2 (Oh *et al.* 2014).

The numeric output of the model can be determined as follow

$$\mathrm{out_i} = \sum_{k=1}^{G} \mathrm{u_{ki}} \mathrm{f_k}(\mathrm{X_i}, \mathrm{v_k}) \tag{11}$$

where u_{ki} is the activation level of the kth fuzzy rule corresponding to ith input pattern.

2.4 Estimating the coefficients of polynomials

As mentioned earlier, the antecedent parts of fuzzy rules are determined by FCM whose results lead to the determination of the membership functions. In consequence part of each fuzzy rule, there are consequent polynomials which their coefficients should be determined. In the design of consequence part, weighted Least Square (WLS) learning algorithm is utilized to estimate the values of the parameters of the polynomials forming the local models. The cost

Table 2 Type and extended forms of polynomials used in the consequent part of fuzzy rule (Oh *et al.* 2014)

Order	Type	Polynomial
1	Constant	$f_k(X_i, v_k) = b_{k0}$
2	Linear	$f_k(X_i, v_k) = b_{k0} + b_{k1}(x_{i1} - v_{k1})$ $+ b_{k2}(x_{i2} - v_{k2}) + \cdots + b_{kn}(x_{in} - v_{kn})$
3	Quadratic	$f_k(X_i, v_k) = b_{k0} + b_{k1}(x_{i1} - v_{k1})$ $+ b_{k2}(x_{i2} - v_{k2}) + \cdots + b_{kn}(x_{in} - v_{kn})$ $+ b_{k(n+1)}(x_{i1} - v_{k1})^2 + b_{k(n+2)}(x_{i2} - v_{k2})^2$ $+ \cdots + b_{k(2n)}(x_{in} - v_{kn})^2$ $+ b_{k(2n+1)}(x_{i1} - v_{k1})(x_{i2} - v_{k2}) + \cdots$ $+ b_{k((n+1)(n+2)/2)}(x_{i(n-1)} - v_{k(n-1)})$ $(x_{in} - v_{kn})$
4	Modified quadratic	$f_k(X_i, v_k) = b_{k0} + b_{k1}(x_{i1} - v_{k1})$ $+ b_{k2}(x_{i2} - v_{k2}) + \cdots + b_{kn}(x_{in} - v_{kn})$ $+ b_{k(n+1)}(x_{i1} - v_{k1})(x_{i2} - v_{k2}) + \cdots$ $+ b_{k(n(n+1)/2)}(x_{i(n-1)} - v_{k(n-1)})(x_{in} - v_{kn})$

function can be expressed as follows (Oh *et al.* 2014)

$$\mathrm{J_L} = \sum_{i=1}^{P} \sum_{k=1}^{G} \mathrm{u_{ki}} (\mathrm{y_k} - \mathrm{f_k}(\mathrm{X_i}, \mathrm{v_k}))^2 \tag{12}$$

The cost function J_L can be expressed in a concise matrix form as follows

$$\mathrm{J_G} = \mathrm{Y} - \mathrm{Xa}^{\mathrm{T}}\mathrm{Y} - \mathrm{Xa} \tag{13}$$

where a is the vector of coefficients of the polynomials, Y is the output vector of data, X is matrix which rearranges input data, centers of each clusters and activation levels. The optimal values of the coefficients of consequent polynomials are determined as follows (Oh *et al.* 2014, Yu and Duan 2013)

$$\mathrm{a} = (\mathrm{X^T X})^{-1} \mathrm{X^T Y} \tag{14}$$

2.5 Biogeography-based optimization (BBO)

Biogeography is the science of the geographical distribution of biological organisms in habitats over time (Zheng *et al.* 2014). It describes how species emigrate and immigrate among habitats, how new species arise, and how species become extinct (1). Simon (2008) developed biogeography-based optimization (BBO) based on the mathematical model of biogeography in which each possible solution of an optimization problem is considered to be analogous to a habitat. In mathematical model of BBO, each solution parameter is denoted as a suitability index variable (SIV) which characterizes the habitability of a habitat. Indeed, each possible solution consists of several SIVs which are the decision variables of the optimization problem. The richness of a habitat is evaluated by the habitat suitability index (HSI) which is similar to the fitness value in other meta-heuristic optimization algorithms (Simon 2008). In BBO, a good solution presents a habitat with a high HSI and the poor solution is similar to a habitat with a low HSI. Due to existence of high organisms in habitats with high HSI values, they have a low immigration and a high emigration rates and it is more probable for them

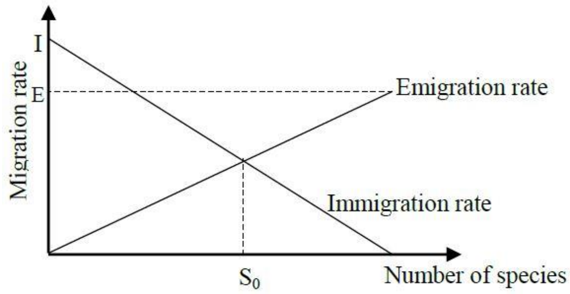

Fig. 3 Relationship between the Number of Species and migration rate (2)

to share their features with poor habitats. Moreover, habitats with low HSI (poor solution) are sparsely populated and have a high immigration and a low emigration rates and they accept features from good solutions. Thus, poor solutions share their features with good solutions with low probabilities. This migration mechanism is very analogous to representatives of a species migrating between fertile habitats and barren habitats (Guo *et al.* 2016). Fig. 3 illustrates a linear model of species distribution in a single habitat, where the immigration rate λ and the emigration rate μ are functions of the HSI value of the habitat. The immigration rate and the emigration rate are functions of the number of species in the habitat. For a single habitat, the immigration rate increases and the emigration rate decreases as the number of species increases. Each habitat has its immigration rate λ_s and emigration rate μ_s. For the straight-line graph of migration, the equations for emigration and immigration rates of a habitat with the number of species s can be calculated as follows (Simon 2008)

$$\lambda_s = I\left(1 - \frac{s}{s_{max}}\right) \tag{15}$$

$$\mu_s = \frac{Es}{s_{max}} \tag{16}$$

where, s_{max} is the largest possible number of species that a habitat can support, I and E are the maximum immigration and emigration rates, respectively.

In BBO, The main procedure is composed of migration and mutation operators. In migration operator, a SIV migrates from an emigrating habitat to an immigrating habitat based on the rates μ and λ of the habitats. The mutation operator randomly modifies a SIV of a habitat according to its a priori probability of existence and tends to raise the diversity of the population (Zheng *et al.* 2014). For low HSI solutions, mutation gives them a chance of improving the quality of solutions, and for high HSI solutions, mutation is able to enhance them even more than they already have (Guo *et al.* 2014, Ma *et al.* 2013). Table 2 presents the basic procedure of BBO, where rand() generates a random real number in the range of [0,1].

2.6 Optimization of FRBFNN using BBO

The performance of the FRBFNN is directly affected by different parameters such as the number of fuzzy rules, the fuzzification coefficient used in the FCM and the polynomial type of consequent part of FRBFNN. The number of fuzzy rules determines the number of sub spaces being used to divide the given entire input space when running the FCM. The fuzzification coefficient influences a degree of overlap between sub spaces. The order of polynomial relates to the type of local model being used to represent sub spaces which are partitioned by means of the FCM (Oh *et al.* 2014). BBO is exploited here to optimize the structure and parameters of the FRBFNN.

As the viewpoint of BBO, the structure of each habitat in FRBFNN consists of three parts. First two parts are related to the antecedent parameters of fuzzy rules while the third part is related to the consequent part of fuzzy rules. The first part involves the number of fuzzy clusters which determines the number of fuzzy rules. It can be between two and the maximum number of rules ($Nrule_{max}$). The second part deals with the fuzzification coefficient which determines the shape of membership functions which ranged between 1 and 3. The third part determines the order of consequent polynomial which can be 1, 2, 3 and 4 for constant, linear, quadratic and modified quadratic polynomials, respectively. Fig. 4 illustrates the arrangement of a habitat in FRBFNN.

Table 2 Pseudo code for basic BBO

```
Begin
    Create a random population of habitats (candidate solutions) H1, H2,...,Hn
    While stop criterion is not satisfied
        Calculate the HSI values of all habitats
        Compute λ and μ of each habitat based on HSI
        For each Hi
            For each SIV of the habitat Hi
                If rand() < λi
                    Select an emigrating habitat Hj with probability α μj
                    Replace the selected SIV of Hi with the corresponding SIV of Hj /*Migration*/
                End if
                If rand() < mutation probability
                    Replace the selected SIV of Hi with a random value /*Mutation*/
                End if
            End for
        End for
    End while
End
```

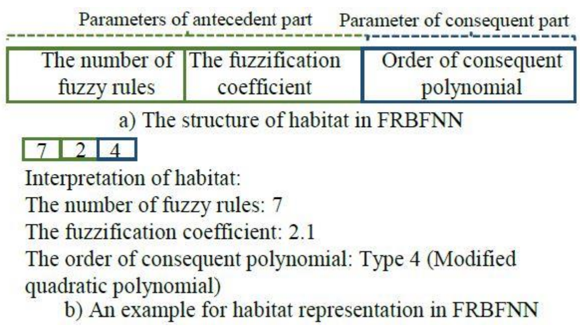

Fig. 4 The structure of habitat and its interpretation in FRBFNN

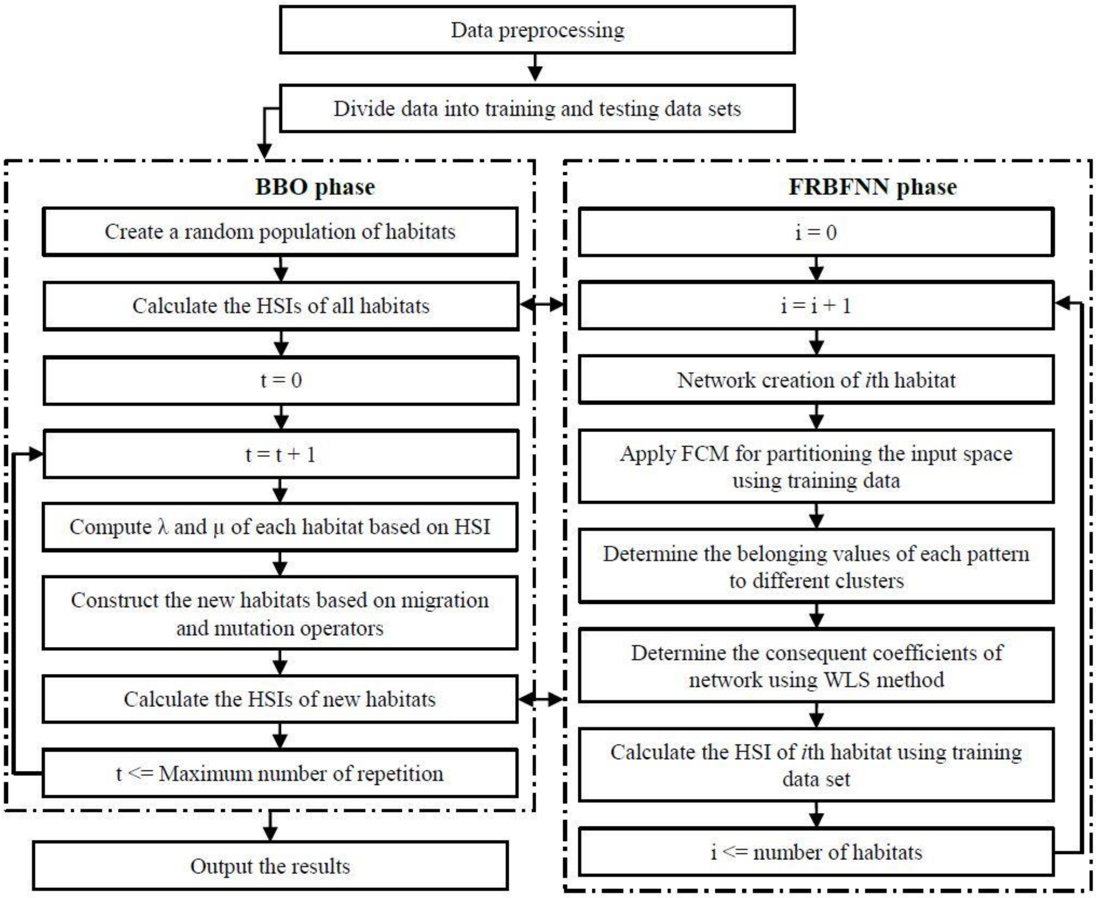

Fig. 5 The learning steps of FRBFNN-BBO algorithm

The detailed learning process of the proposed FRBFNN-BBO model is illustrated in Fig. 5 and the main steps comprises the following steps.

Step 1: Data preprocessing

The data preprocessing can prevent the saturation problem and consequently the low rate of the training. Before the training of the model, both input and output variables are linearly normalized in the range [-1, 1] using minimax algorithm from the following equation

$$\mathrm{x_n} = \frac{2 \times (\mathrm{x} - \mathrm{x_{min}})}{(\mathrm{x_{max}} - \mathrm{x_{min}})} - 1 \tag{17}$$

where x, x_n, $x_{\max}$ and $x_{\min}$ are the actual, normalized, maximum and minimum values of input or output data, respectively.

Step 2: Division of data into training and testing data

All input-output data set is randomly split into the training and testing sets. Training data is used to construct the FRBFNN-BBO model and testing data is applied to validate the quality of the proposed model.

Step 3: Construction of the random habitats

As stated earlier, the structure of the FRBFNN-BBO model including the number of fuzzy rules, the fuzzification coefficient and the order of consequent polynomial is determined using BBO algorithm. In this regard, according to Fig. 4, the structure of each habitat consists of three SIVs. At the beginning, all habitats are randomly generated considering the lower and upper bounds of each SIV.

Step 4: Training phase

For each habitat, the FCM is used to partition the input space based on the values of first and second SIVs and the value of third SIV determines the polynomial order of the consequent part. Therefore, the architecture of FRBFNN related to each habitat is specified, the coefficients of polynomial calculated according to Eqs. (12)-(14) and the performance of each habitat is evaluated using the root mean squared error (RMSE) value as follow

$$\mathrm{RMSE_{H_k}} = \sqrt{\frac{1}{\mathrm{P}}\sum_{\mathrm{i=1}}^{\mathrm{P}}(\mathrm{T_i} - \mathrm{O_i})^2} \tag{18}$$

$$\mathrm{HSI}_{\mathrm{H}_k} = \frac{1}{1 + \mathrm{RMSE}_{\mathrm{H}_k}} \tag{19}$$

where $RMSE_{H_k}$ and $\mathrm{HSI_{H_k}}$ are, respectively, the RMSE and HSI of the kth habitat, P is the number of data and T_i, O_i and are the target value and the model output of ith data, respectively.

Step 5: Application of BBO

According to the obtained HSIs for all habitats, the values of λ and μ of all habitats are calculated and the new habitats are acquired according to the migration and mutation processes of BBO algorithm mentioned in Sec. 3.

Step 6: Check the termination criterion.

Table 3 Descriptive statistics of the input and output parameters

Data type	Statistical Parameters	*C* (Kg/m^3)	*W* (Kg/m^3)	*CAgg* (Kg/m^3)	*FAgg* (Kg/m^3)	FA (Kg/m^3)	SP (%)	*A* (Days)	f_c (MPa)
All data	Min	61	135.45	590	434	20	0	1	3.996
	Max	583	295.2	1190	1109	427.5	4.6	365	107.46
	Ave	302.61	192.18	815.12	814.58	172.69	1.07	41.07	35.08
	S.D.	101.70	31.24	124.69	121.80	72.92	1.09	62.90	19.31
Training data	Min	61	135.45	590	434	20	0	1	3.996
	Max	583	295.2	1190	1109	427.5	4.6	365	104.85
	Average	304.30	192.36	813.43	813.77	171.75	1.10	42.36	35.15
	S.D.	101.39	30.32	127.42	124.10	74.79	1.11	64.62	19.18
Testing data	Min	61	135.45	590	478	50	0	1	5
	Max	583	295.2	1058.2	1109	373	4.6	365	107.46
	Average	295.90	191.46	821.81	817.81	176.41	0.95	35.91	34.78
	S.D.	103.39	34.89	113.86	113.00	65.33	1.00	55.68	19.96

If the termination criterion of BBO algorithm is not satisfied, step 4 with new generated habitats and step 5 should be repeated. Otherwise, the process of FRBFNN-BBO algorithm has been completed and the habitat with the best fitness is selected and the corresponding parameters reported as the optimal FRBFNN.

3. Model development

3.1 Data preparation

The amount of data used for developing the proposed algorithm has a crucial impact on its reliability. In this study, a comprehensive dataset contains the total number of 338 experimental results were gathered from different literature to train and validate the reliability of the proposed algorithm for predicting the compressive strength of SCC containing fly ash (Bingöl and Tohumcu 2013, Bouzoubaâ and Lechami 2001, Bui *et al.* 2002, Chabib and Syed 2012, Concrete *et al.* 2004, Gesoğlu and Ö zbay 2007, Güneyisi *et al.* 2010, 2015, Khatib 2008, Le and Ludwig 2016, Leung *et al.* 2016, Liu 2010, Mohamed 2011, Pathak and Siddique 2012, Pofale and Deo 2010, Şahmaran *et al.* 2011, Siad *et al.* 2014, Siddique *et al.* 2012, da Silva *et al.* 2015, Sonebi 2004, Sonebi and Cevik 2009b, Sukumar *et al.* 2008, Ulucan *et al.* 2008, Zhao *et al.* 2015). The constituents of concrete including cement (C), water (W), coarse aggregate (CAgg), fine aggregate (FAgg), fly ash (FA) and superplasticizer (SP) in addition to the concrete age (A) were considered as input parameters of model and the concrete compressive strength (f_c) was assumed as output parameter. 80% of all data, i.e., 270 samples, was randomly selected as training data to construct the fuzzy rules and tuning of the polynomial coefficients of consequent parts, while 20% of remaining data, i.e., 68 samples, was chosen to investigate the performance of the developed model for unknown patterns. All training and testing data are given in the Appendix section at the end of the paper. In addition, the descriptive statistics of the input and output parameters including minimum (Min), maximum (Max), average (Ave) and standard deviation (S.D.) for training, testing and all datasets are given in Table 3.

Table 4 Adjustable parameters of the proposed model

Number of habitats	50
Kept percentage of habitats from previous population in new generation	20%
Mutation probability	0.1
Maximum number of cycles of BBO algorithm	100
Number of rules	Between 2 and10
Range of fuzzification coefficient	Between 1 and 3

Table 5 The optimal fuzzy cluster centers of antecedent parts of fuzzy rules

Rule No.	Fuzzy cluster centers
Rule 1	(-0.4150, -0.6810, -0.1630, -0.0680, 0.2940, -0.7660, -0.8980)
Rule 2	(-0.3880, -0.4200, 0.2400, -0.2740, 0.0820, -0.7500, -0.8080)
Rule 3	(-0.2210, -0.1190, -0.2680, -0.1850, 0.0280, -0.6910, -0.6610)
Rule 4	(-0.2060, 0.5560, -0.1680, -0.1770, -0.4860, -0.7790, -0.7380)
Rule 5	(-0.0030, -0.4140, -0.3930, -0.1190, 0.0930, -0.6860, -0.8150)
Rule 6	(0.0560, -0.3170, -0.5260, -0.9190, 0.9750, 0.9680, -0.9040)
Rule 7	(0.0600, -0.3090, -0.2870, -0.5180, 0.3580, -0.4400, -0.8520)
Rule 8	(0.0730, -0.5390, -0.4460, 0.5440, -0.3290, -0.7690, -0.8120)
Rule 9	(0.3480, 0.1790, -0.4350, -0.9140, 0.4050, 0.5630, -0.8640)
Rule 10	(0.6390, -0.2620, -0.6060, -0.4280, 0.1130, -0.6760, -0.8630)

3.2 Development of FRBFNN-BBO for predicting the compressive strength of SCC with fly ash

The FRBFNN-BBO model developed herein is mainly aimed to generate an artificial intelligence method for predicting the compressive strength of SCC containing fly ash. Behavior modeling of the compressive strength of SCC containing fly ash is essentially more difficult than conventional concrete. In this study, the FRBFNN-BBO approach is utilized to obtain the hidden relationships between the compressive strength of SCC mixes and the influencing variables as follows

$$f_c = g(C, W, CAgg, FAgg, FA, SP, A) \tag{20}$$

The proposed FRBFNN-BBO algorithm was created, trained and implemented in MATLAB environment. There are some adjustable parameters which should be fixed before implementation of the proposed model which are given in Table 4.

After running the developed model in MATLAB, the results showed that the optimum number of fuzzy rules, fuzzification coefficient and the polynomials used in the consequent part of fuzzy rules are, respectively, 10, 1.7658 and quadratic. The optimal values of fuzzy cluster centers in the antecedent parts and the optimal coefficients of polynomials in the consequent parts of fuzzy rules are given in Tables 5 and 6, respectively.

Table 6 The optimal coefficients of final polynomials in the consequent parts of fuzzy rules

Rule No.	Rule 1	Rule 2	Rule 3	Rule 4	Rule 5	Rule 6	Rule 7	Rule 8	Rule 9	Rule 10
Constant	-0.0255	-0.0255	-0.0255	-0.0255	-0.0255	-0.0255	-0.0255	-0.0255	-0.0255	-0.0255
$(x_{i1}-v_{k1})$	-0.5495	1.2303	1.3073	-1.4558	3.1210	0.6170	-1.6561	1.5282	-0.5824	5.0858
$(x_{i2}-v_{k2})$	1.2582	1.9625	-2.4970	-1.0790	1.2965	0.1276	-1.5658	-4.1587	0.3408	-2.3461
$(x_{i3}-v_{k3})$	-1.1144	-1.8558	-3.9318	-0.1592	0.9264	0.9133	-2.0347	0.6610	0.3604	3.5212
$(x_{i4}-v_{k4})$	3.4291	-3.0786	1.2945	-0.9178	1.8703	2.2934	0.6350	2.1856	-1.2128	-2.3096
$(x_{i5}-v_{k5})$	-1.4438	-1.9573	-2.1143	-1.4222	-1.0878	-3.7935	0.1407	-1.1990	-0.3132	1.5808
$(x_{i6}-v_{k6})$	-0.0690	-0.9024	2.5090	-2.8126	-3.4976	-6.4773	-3.0142	3.6621	-3.1313	-0.5611
$(x_{i7}-v_{k7})$	3.9977	1.1614	1.3715	0.5797	0.0464	1.5708	3.2235	0.5530	1.6583	3.6127
$(x_{i1}-v_{k1})^2$	0.5325	1.8104	1.1154	-3.4039	0.0855	-0.8155	-0.7838	0.6471	-1.5878	-1.8148
$(x_{i2}-v_{k2})^2$	2.9437	-2.4687	0.5052	-0.3901	2.6075	-2.7650	3.2808	0.1208	-0.5349	1.8388
$(x_{i3}-v_{k3})^2$	3.6402	0.9215	-1.2474	-2.5732	7.3876	-2.8688	1.4386	1.7247	-0.7183	-0.5678
$(x_{i4}-v_{k4})^2$	1.2565	-2.1776	-3.7625	-0.9712	1.7890	-0.9766	-2.7733	-2.3897	-2.3674	-0.3069
$(x_{i5}-v_{k5})^2$	-0.0289	2.8314	-3.7083	1.0609	2.0007	-1.7952	-0.4363	-0.7262	0.3953	1.5452
$(x_{i6}-v_{k6})^2$	-4.3753	4.5996	2.0592	-1.5241	-0.6278	-4.1728	1.2648	0.2695	-4.0756	5.5029
$(x_{i7}-v_{k7})^2$	-7.8344	-3.7901	11.5061	0.0327	-14.5906	4.7811	-1.6869	3.8903	5.1930	-9.3235
$(x_{i1}-v_{k1})(x_{i2}-v_{k2})$	2.8139	-3.2122	3.3304	5.9017	2.4219	-0.7495	1.7169	3.1533	-2.2001	1.7888
$(x_{i1}-v_{k1})(x_{i3}-v_{k3})$	-1.9761	-0.7617	-0.3581	2.3464	-0.3088	-0.1521	-1.8046	-1.8807	2.2330	-3.2321
$(x_{i1}-v_{k1})(x_{i4}-v_{k4})$	-0.5384	1.9200	-0.0339	1.3709	4.0562	-0.0501	3.2315	-0.4844	1.4998	5.4090
$(x_{i1}-v_{k1})(x_{i5}-v_{k5})$	4.9592	-3.9649	3.0163	-3.0251	-2.9297	1.2294	-2.3744	-2.1548	2.0466	-0.7944
$(x_{i1}-v_{k1})(x_{i6}-v_{k6})$	1.9732	7.4949	-0.7736	-3.0518	-1.1358	2.0301	-1.4277	-1.3080	0.6736	-2.3277
$(x_{i1}-v_{k1})(x_{i7}-v_{k7})$	6.5880	0.5040	0.4200	-0.0959	-7.8565	0.6806	9.8472	7.2675	0.9466	8.3021
$(x_{i2}-v_{k2})(x_{i3}-v_{k3})$	-0.8003	5.1647	-1.0484	-1.6594	0.1740	-3.1326	2.8900	-2.2098	0.6983	2.1176
$(x_{i2}-v_{k2})(x_{i4}-v_{k4})$	0.8353	-3.8485	0.3845	1.3536	-2.9822	0.6652	0.4778	-0.3074	1.9301	0.9074
$(x_{i2}-v_{k2})(x_{i5}-v_{k5})$	2.3758	-2.3683	-3.0424	0.7360	2.7591	2.3086	-3.9067	1.9345	-0.5800	1.1742
$(x_{i2}-v_{k2})(x_{i6}-v_{k6})$	-0.2235	-1.5340	-3.7296	1.7217	-2.0129	0.8935	-2.6617	-0.8424	-0.3448	0.3119
$(x_{i2}-v_{k2})(x_{i7}-v_{k7})$	-0.3432	7.8741	-5.0264	-0.7081	-2.0140	-3.9695	0.8434	-2.1865	-6.4038	8.5411
$(x_{i3}-v_{k3})(x_{i4}-v_{k4})$	3.8607	1.4984	1.6856	0.9479	-2.2503	-0.0299	-2.9105	3.1035	-0.5389	-2.9534
$(x_{i3}-v_{k3})(x_{i5}-v_{k5})$	-4.1850	-1.5500	2.7579	-1.2897	-0.0242	2.6816	0.0111	0.0840	0.4265	2.5740
$(x_{i3}-v_{k3})(x_{i6}-v_{k6})$	-1.0899	0.1320	1.8652	-0.6908	-0.6225	2.1403	0.9720	1.7333	-1.4140	-1.8441
$(x_{i3}-v_{k3})(x_{i7}-v_{k7})$	7.8739	-2.4285	-4.0010	2.2894	-5.0156	2.6258	7.8618	7.2778	1.6222	-0.9196
$(x_{i4}-v_{k4})(x_{i5}-v_{k5})$	-5.2989	2.0577	-0.7678	-1.0385	-3.9176	1.0673	1.1136	-0.0665	-1.0256	-4.3317
$(x_{i4}-v_{k4})(x_{i6}-v_{k6})$	-3.0529	-0.4206	3.2220	-1.0731	0.1263	1.6319	3.3454	-3.1949	3.4092	0.2113
$(x_{i4}-v_{k4})(x_{i7}-v_{k7})$	5.0770	-0.0217	3.7000	0.0163	-3.3707	4.8738	6.8848	-4.9722	6.5339	-2.0371
$(x_{i5}-v_{k5})(x_{i6}-v_{k6})$	-0.5063	-2.2806	-0.7153	1.0502	0.9627	-2.8693	-0.9333	2.6994	0.1535	0.6726
$(x_{i5}-v_{k5})(x_{i7}-v_{k7})$	3.3038	3.3006	-2.9984	2.4445	-4.5064	-1.8587	-4.0037	-0.5739	-1.5082	10.8545
$(x_{i6}-v_{k6})(x_{i7}-v_{k7})$	5.9154	-2.1734	-0.9709	3.4535	1.5829	-5.7664	21.199	-1.1053	0.4577	-6.1777

Table 7 Statistical parameters of the different developed models

	FRBFNN-BBO		ANN		1^{st} RBFNN model		2^{st} RBFNN model		3^{st} RBFNN model	
Statistical parameters	Training data	Testing data	Training data	Testing data	Training data	Testing data	Training data	Testing data	Training data	Testing data
RMSE (MPa)	3.4053	5.8496	4.6361	9.8555	9.9332	16.5661	10.7275	13.5696	9.3128	13.6373
MAE (MPa)	2.3577	4.6347	3.4984	7.8352	7.8719	11.1898	8.4781	10.3031	7.1228	9.9774
MAPE (%)	10.5945	17.8321	14.0294	22.2462	36.9886	37.3674	37.99	36.0096	32.0296	37.8084
R-value	0.9840	0.9614	0.9644	0.9088	0.8238	0.6764	0.7907	0.7998	0.8471	0.7744
OBJ	3.8868		6.2038		12.4962		11.7465		10.6726	

4. Results and discussion

In order to investigate the performance of the FRBFNN-BBO model, the accuracy of the proposed model was compared with that of other four artificial intelligence models. In this regard, an ANN model and three RBFNN models were developed, trained and tested under the MATLAB program. In the case of ANN, a feed-forward back-propagation neural network with one hidden layer was considered and the levenberg-marquardt algorithm (Hagan and Menhaj 1994) was used for its training. The number of neurons in the hidden layer was calculated equal to six which was determined by try and error method. In the first RBFNN model, the centers of RBFs were chosen among the input vectors of the training data. At the beginning, there was no RBF in the hidden layer and in each step a training vector with the smallest measure of correlation with the target was added to the hidden layer. These steps were repeated until one of the termination conditions of the algorithm was satisfied. In the second and third RBFNN models, crisp clustering method, called *k*-means clustering (Hartigan and Wong 1979), and fuzzy *c*-mean clustering were used for calculating the centers of RBFs, respectively. In all RBFNN models, the weights of second layer were determined using the least mean square (LMS) method. In addition, Gaussian RBFs were considered for all three models and the number of RBFs in the hidden layer was limited to ten. Moreover, the spread of RBFs was considered equal to the maximum distance between any two centers of RBFs divided to the square root of centers' number.

For comparing the efficiency of different developed models, it is crucial to define the criteria, which show their performances and accuracies. Several statistical parameters such as root mean squared error (RMSE), mean absolute error (MAE), mean absolute percentage error (MAPE) and correlation coefficient (R) were used. Moreover, in order to consider the simultaneous effect of different statistical parameters, another parameter, namely OBJ, was also calculated (Gandomi *et al.* 2013). The above-mentioned parameters are defined below (Golafshani and Ashour 2016a).

$$\mathrm{RMSE} = \sqrt{\frac{\sum_{i=1}^{N}(T_i - O_i)^2}{N}} \tag{21}$$

$$\mathrm{MAE} = \frac{1}{N}\sum_{i=1}^{N}|T_i - O_i| \tag{22}$$

$$\mathrm{MAPE} = \frac{100}{N}\sum_{i=1}^{N}\frac{|T_i - O_i|}{O_i} \tag{23}$$

$$R = \frac{\sum_{i=1}^{N}(T_i - \bar{T}_i)(O_i - \bar{O}_i)}{\sqrt{\sum_{i=1}^{N}(T_i - \bar{T}_i)^2 \sum_{i=1}^{N}(O_i - \bar{O}_i)^2}} \tag{24}$$

$$\mathrm{OBJ} = \left(\frac{No._{Train} - No._{Test}}{No._{Train} + No._{Test}}\right)\frac{\mathrm{RMSE}_{Train} + \mathrm{MAE}_{Train}}{R_{Train} + 1} + \left(\frac{2No._{Test}}{No._{Train} + No._{Test}}\right)\frac{\mathrm{RMSE}_{Test} + \mathrm{MAE}_{Test}}{R_{Test} + 1} \tag{25}$$

where T_i, O_i are, respectively, the actual and predicted output of *i*th pattern and N, $No._{Train}$ and $No._{Test}$ are the total numbers of patterns in dataset, training data and testing data, respectively. In addition, $\bar{T}_i$ and $\bar{O}_i$ present the average of actual and predicted outputs, respectively. If the RMSE value is small, the results obtained from the models are closer to the experimental results. On the other hand, if the RMSE value is high, the results obtained by the models are far from the experimental results. If R values are above 0.8, and also closer to 1, the results obtained from the models are more linearly correlated with the experimental results. The total errors between the experimental results and model results are also evaluated by using the MAPE statistical value. In addition, the mean absolute errors between each experimental result and model results are determined by using the MAE statistical value.

The statistical parameters of the training and testing sets of different models are given in the Table 7. As seen in this Table, the RMSE, MAE, MAPE and R values of the proposed model for training data are 3.4053 MPa, 2.3577 MPa, 10.5945% and 0.9840, respectively, while these values are, respectively, 5.8496 MPa, 4.6347 MPa, 17.8321% and 0.9614 for testing data. As can be seen, there is a close harmony between the developed model's predictions and experimental results. In addition, the OBJ value of the FRBFNN-BBO model is much lower than other models. It is nearly 63%, 31%, 33% and 36% of the OBJ values of ANN, first, second and third RBFNN models, respectively. It proves that the proposed FRBFNN-BBO model considerably outperforms than other models. In Comparison with all three RBFNN models, the accuracy of the developed ANN model is much better. Moreover, the efficiency of third RBFNN model is better than the first and second RBFNN models. Although the performance differences of three RBFNN models are negligible, the results demonstrate that the fuzzy c-mean clustering can determine the centers of RBFs more effectively.

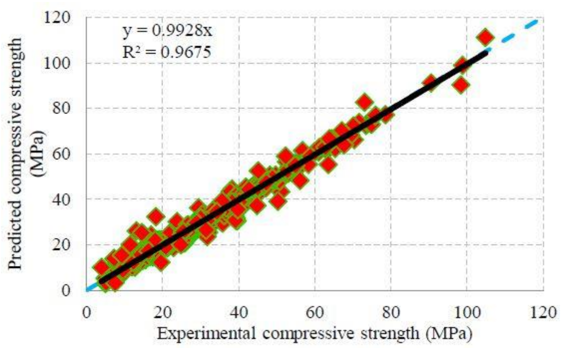

(a)

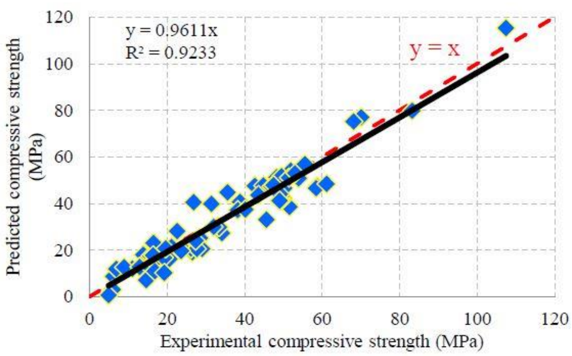

(b)

Fig. 6 Predicted versus experimental compressive strength for (a) training (b) testing datasets

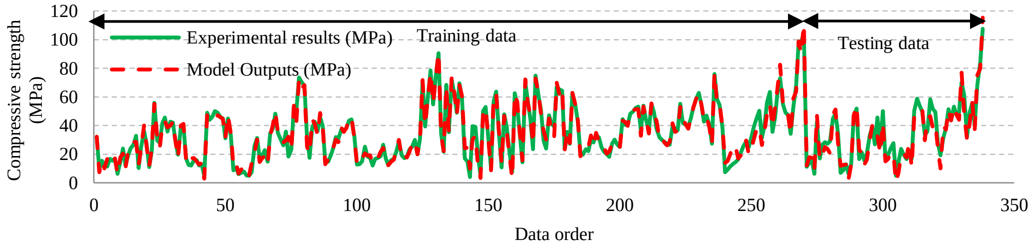

Fig. 7 The comparison of the predicted and experimental compressive strength for training and testing datasets

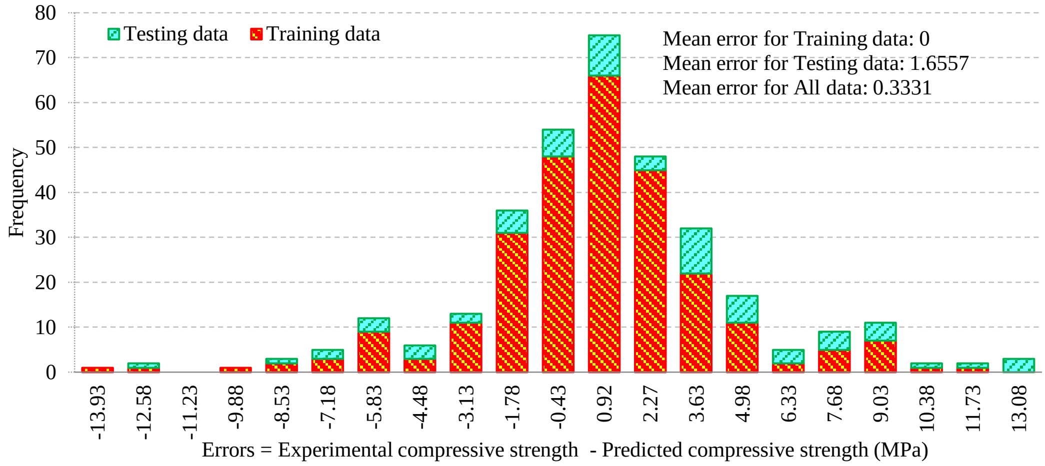

Fig. 8 Error histogram for both training and testing datasets

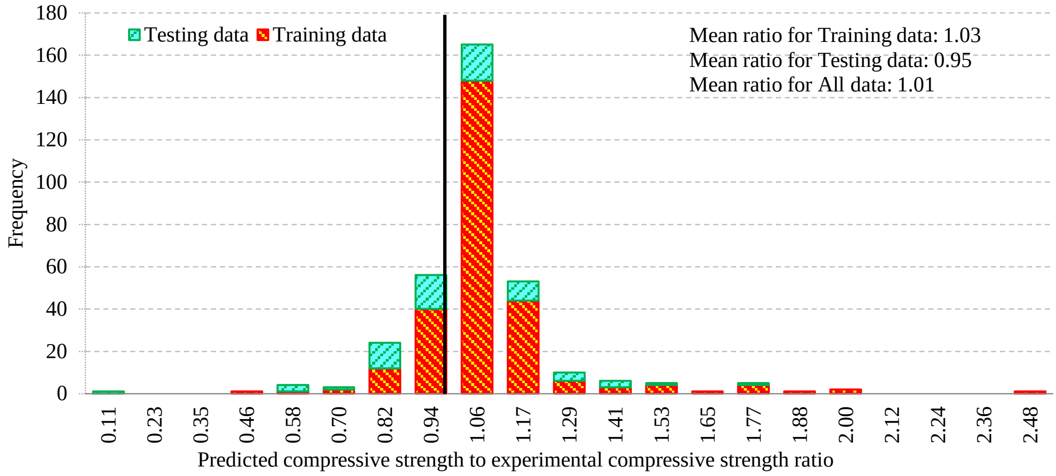

Fig. 9 A comparison of the ratio of the predicted to experimental compressive strength values using histogram

Fig. 6 illustrates the relations between the predictions made by the developed model and the experimental compressive strength of SCC containing fly ash for both training and testing data, respectively.

Comparing the proposed model's predictions with the experimental results for the training dataset shows a high learning capability of the proposed model with reasonable error and high correlation. Moreover, the testing dataset results demonstrate that the proposed model has comparatively low error values with considerably high generalization capacity.

The predicted compressive strengths of SCC containing fly ash achieved through the proposed FRBFNN-BBO model are compared with the experimental results in Fig. 7. It is observed that the proposed FRBFNN-BBO model is able to closely follow trend seen in the experimental data for both training and testing sets.

The error histogram of both training and testing datasets is shown in Fig. 8. As illustrated in this figure, the mean error values for training, testing and all data are, respectively, 0, 1.6557 and 0.3331 MPa and the error distribution around zero value is high for both data sets. It indicates that the performance of the developed model is desirable with reasonable error.

The ratio of the predicted to experimental compressive strength values made by the proposed FRBFNN-BBO model for both training and testing data are visualized in Fig. 9. A model has good prediction precision if the ratio of the predicted to experimental compressive strength is equal or near to one. As can be observed from this figure, the distribution frequency of the ratio of the predicted to experimental compressive strength for the developed model has a mode close to one. The mean values of this ratio are 1.03 and 0.95 for training and testing data, respectively. Thus, the proposed model significantly outperforms in predicting the compressive strength of SCC containing fly ash.

5. Conclusions

Because of the non-homogenous constituents of SCC containing fly, prediction of its compressive strength is a difficult and complicated task. Artificial intelligent-based methods are known as robust tools for modeling of complex systems. In this paper, the hybridization of one nature inspired computational techniques i.e. biogeography-based optimization (BBO) and fuzzy radial basis function neural network (FRBFNN) has been proposed as a new artificial intelligence method (FRBFNN-BBO) and this attractive method was applied for estimating the compressive strength of SCC containing fly ash. For comparison purpose, an ANN model and three different RBFNN models were developed and their performances were compared with the proposed model. The following conclusions are obtained from this study:

- The proposed FRBFNN-BBO model is a practicable method with reasonable error for predicting the compressive strength of SCC containing fly ash. The mean error, the average predicted compressive strength to experimental compressive strength ratio and R- value equal to 1.6557 MPa, 0.95 and 0.9614 for testing data exhibit a successful performance of the FRBFNN-BBO model.
- Comparison between the FRBFNN-BBO model and all other developed models in terms of statistical parameters showed that the proposed model provides much better results than all other models' results.
- The correlation coefficients of the developed ANN model were more than 0.9 for both training and testing data and the ANN model well agreed with the experimental data. Moreover, it outperforms considerably the developed RBFNN models.
- Although the efficiencies of different developed RBFNN models are lower than the proposed FRBFNN-BBO and the developed ANN models in this study, but it can be concluded that fuzzy c-mean clustering algorithm is a suitable method for calculating the centers of radial basis functions in RBFNN models.

References

Aiyer, B.G., Kim, D., Karingattikkal, N., Samui, P. and Rao, P.R. (2014), "Prediction of compressive strength of self-compacting concrete using least square support vector machine and relevance vector machine", *KSCE. J. Civil Eng.*, **18**(6), 1753-1758.

Ashteyat, A.M. and Ismeik, M. (2018), "Predicting residual compressive strength of self-compacted concrete under various temperatures and relative humidity conditions by artificial neural networks", *Comput. Concrete*, **21**(1), 47-54.

Atici, U. (2011), "Prediction of the strength of mineral admixture concrete using multivariable regression analysis and an artificial neural network", *Exp. Syst. Appl*., **38**(8), 9609-9618.

Baykasoğlu, A., Öztaş, A. and Özbay, E. (2009), "Prediction and multi-objective optimization of high-strength concrete parameters via soft computing approaches", *Exp. Syst. Appl*., **36**(3), 6145-6155.

Behnood, A. and Golafshani, E.M. (2018), "Predicting the compressive strength of silica fume concrete using hybrid artificial neural network with multi-objective grey wolves", *J. Clean. Prod*., **202**, 54-64.

Bilim, C., Atiş, C.D., Tanyildizi, H. and Karahan, O. (2009), "Predicting the compressive strength of ground granulated blast furnace slag concrete using artificial neural network", *Adv. Eng. Softw*., **40**(5), 334-340.

Bingöl, A.F. and Tohumcu, I. (2013), "Effects of different curing regimes on the compressive strength properties of self-compacting concrete incorporating fly ash and silica fume", *Mater. Des*., **51**, 12-18.

Boğa, A.R., Öztürk, M. and Topçu, I.B. (2013), "Using ANN and ANFIS to predict the mechanical and chloride permeability properties of concrete containing GGBFS and CNI", *Compos. Part B. Eng*., **45**(1), 688-696.

Bouzoubaâ, N. and Lachemi, M. (2001), "Self Compacting Concrete Incorporating High-Volumes of Class F Fly Ash : Preliminary Results", *Cement Concrete Res*., **31**(3), 413-420.

Bui, D.K., Nguyen, T., Chou, J.S., Nguyen-Xuan, H. and Ngo, T.D. (2018), "A modified firefly algorithm-artificial neural network expert system for predicting compressive and tensile strength of high-performance concrete", *Constr. Build. Mater*., **180**(20), 320-333.

Bui, V.K., Akkaya, Y. and Shah, S.P. (2002), "Rheological model for self-consolidating concrete", *ACI. Mater. J*., **99**(6), 549-559.

Castelli, M., Vanneschi, L. and Silva, S. (2013), "Prediction of high performance concrete strength using Genetic Programming with geometric semantic genetic operators", *Exp. Syst. Appl*., **40**(17), 6856-6862.

Chabib, H. El and Syed, A. (2012), "Properties of self-consolidating concrete made with high volumes of supplementary cementitious materials", *J. Mater. Civil Eng*., **25**(11), 1579-1586.

Cheng, M.Y., Chou, J.S., Roy, A.F.V. and Wu, Y.W. (2012), "High-performance concrete compressive strength prediction using time-weighted evolutionary fuzzy support vector machines inference model", *Autom. Constr*., **28**, 106-115.

Cheng, M.Y., Firdausi, P.M. and Prayogo, D. (2014), "High-performance concrete compressive strength prediction using Genetic Weighted Pyramid Operation Tree (GWPOT)", *Eng. Appl. Artif. Intell*., **29**, 104-113.

Chou, J.S. and Pham, A.D. (2013), "Enhanced artificial intelligence for ensemble approach to predicting high performance concrete compressive strength", *Constr. Build. Mater*., **49**, 554-563.

da Silva, P.R. and de Brito, J. (2015), "Experimental study of the porosity and microstructure of self-compacting concrete (SCC) with binary and ternary mixes of fly ash and limestone filler", *Constr. Build. Mater*., **86**, 101-112.

El-Dieb, A.S. and Reda Taha, M.M. (2012), "Flow characteristics and acceptance criteria of fiber-reinforced self-compacted concrete (FR-SCC)", *Constr. Build. Mater*., **27**(1), 585-596.

Gandomi, A.H., Yun, G.J. and Alavi, A.H. (2013), "An evolutionary approach for modeling of shear strength of RC deep beams", *Mater. Struct*., **46**(12), 2109-2119.

Gesoğlu, M. and Özbay, E. (2007), "Effects of mineral admixtures on fresh and hardened properties of self-compacting concretes: binary, ternary and quaternary systems", *Mater. Struct*., **40**(9), 923-937.

Ghezal, A. and Khayat, K.H. (2002), "Optimizing self-consolidating concrete with limestone filler by using statistical factorial design methods", *ACI. Mater. J*., **99**(3), 264-272.

Gilan, S.S., Jovein, H.B. and Ramezanianpour, A.A. (2012), "Hybrid support vector regression-Particle swarm optimization for prediction of compressive strength and RCPT of concretes containing metakaolin", *Constr. Build. Mater*., **34**, 321-329.

Golafshani, E.M. and Ashour, A. (2016a), "A feasibility study of BBP for predicting shear capacity of FRP reinforced concrete beams without stirrups", *Adv. Eng. Softw*., **97**, 29-39.

Golafshani, E.M. and Ashour, A. (2016b), "Prediction of self-compacting concrete elastic modulus using two symbolic regression techniques", *Autom. Constr*., **64**, 7-19.

Golafshani, E.M., Rahai, A. and Sebt, M.H. (2014), "Bond behavior of steel and GFRP bars in self-compacting concrete", *Constr. Build. Mater*., **61**, 230-240.

Güneyisi, E., Gesoglu, M., Al-Goody, A. and Ipek, S. (2015), "Fresh and rheological behavior of nano-silica and fly ash blended self-compacting concrete", *Constr. Build. Mater*., **95**, 29-44.

Güneyisi, E., Gesolu, M. and Özbay, E. (201), "Strength and drying shrinkage properties of self-compacting concretes incorporating multi-system blended mineral admixtures", *Constr. Build. Mater*., **24**(10), 1878-1887.

Guo, W., Wang, L. and Wu, Q. (2014), "An analysis of the migration rates for biogeography-based optimization", *Inform. Sci*., **254**, 111-140.

Guo, W., Wang, L. and Wu, Q. (2016), "Numerical comparisons of migration models for Multi-objective Biogeography-Based Optimization", *Inf. Sci*., **328**, 302-320.

Hagan, M.T. and Menhaj, M.B. (1994), "Training feedforward networks with the marquardt algorithm", *IEEE Tran. Neural Netw.*, **5**(6), 989-993.

Hartigan, J.A. and Wong, M.A. (1979), "Algorithm AS 136: A K-means clustering algorithm", *Appl. Stat*., **28**(1), 100-108.

Ivakhnenko, A.G. (1971), "Polynomial Theory of Complex Systems", *IEEE Tran. Syst. Man. Cybern*., **SMC-1**(4), 364-378.

Khan, M.I. (2012), "Predicting properties of High Performance Concrete containing composite cementitious materials using Artificial Neural Networks", *Autom. Constr*., **22**, 516-524.

Khatib, J.M. (2008), "Performance of self-compacting concrete containing fly ash", *Constr. Build. Mater*., **22**(9), 1963-1971.

Krishnasamy, U. and Nanjundappan, D. (2016), "Hybrid weighted probabilistic neural network and biogeography based optimization for dynamic economic dispatch of integrated multiple-fuel and wind power plants", *Int. J. Electr. Power. Energy Syst*., **77**, 385-394.

Le, H.T. and Ludwig, H.M. (2016), "Effect of rice husk ash and other mineral admixtures on properties of self-compacting high performance concrete", *Mater. Des*., **89**, 156-166.

Leung, H.Y., Kim, J., Nadeem, A., Jaganathan, J. and Anwar, M.P. (2016), "Sorptivity of self-compacting concrete containing fly ash and silica fume", *Constr. Build. Mater*., **113**, 369-375.

Liu, M. (2010), "Self-compacting concrete with different levels of pulverized fuel ash", *Constr. Build. Mater*., **24**(7), 1245-1252.

Ma, H., Simon, D., Fei, M. and Xie, Z. (2013), "Variations of biogeography-based optimization and Markov analysis", *Inform. Sci*., **220**, 492-506.

Mantas, C.J. and Puche, J.M. (2008), "Artificial neural networks are zero-order TSK fuzzy systems", *IEEE Tran. Fuzzy Syst*., **16**(3), 630-643.

Mashhadban, H., Kutanaei, S.S. and Sayarinejad, M.A. (2016), "Prediction and modeling of mechanical properties in fiber reinforced self-compacting concrete using particle swarm optimization algorithm and artificial neural network", *Constr. Build. Mater*., **119**, 277-287.

Melo, K.A. and Carneiro, A.M.P. (2010), "Effect of Metakaolin's finesses and content in self-consolidating concrete", *Constr. Build. Mater*., **24**(8), 1529-1535.

Mitra, S. and Basak, J. (2001), "FRBF: A fuzzy radial basis function network", *Neur. Comput. Appl*., **10**(3), 244-252.

Mohamed, H.A. (2011), "Effect of fly ash and silica fume on compressive strength of self-compacting concrete under different curing conditions", *Ain Shams Eng. J*., **2**(2), 79-86.

Mousavi, S.M., Aminian, P., Gandomi, A.H., Alavi, A.H. and Bolandi, H. (2012), "A new predictive model for compressive strength of HPC using gene expression programming", *Adv. Eng. Softw*., **45**(1), 105-114.

Oh, S.K., Kim, W.D., Pedrycz, W. and Seo, K. (2014), "Fuzzy radial basis function neural networks with information granulation and its parallel genetic optimization", *Fuzzy Set. Syst*., **237**, 96-117.

Ozawa, K., Maekawa, K. and Okamura, H. (1990), "High performance concrete with high filling ability", *Proceedings of the RILEM Symposium, Admixtures for Concrete*, Barcelona.

Ozbay, E., Gesoglu, M. and Güneyisi, E. (2008), "Empirical modeling of fresh and hardened properties of self-compacting concretes by genetic programming", *Constr. Build. Mater*., **22**(8), 1831-1840.

Özcan, F., Atiş, C.D., Karahan, O., Uncuoğlu, E. and Tanyildizi, H. (2009), "Comparison of artificial neural network and fuzzy logic models for prediction of long-term compressive strength of silica fume concrete", *Adv. Eng. Softw*., **40**(9), 856-863.

Öztaş, A., Pala, M., Özbay, E., Kanca, E., Çaglar, N. and Bhatti, M.A. (2006), "Predicting the compressive strength and slump of high strength concrete using neural network", *Constr. Build. Mater*., **20**(9), 769-755.

Pala, M., Özbay, E., Öztaş, A. and Yuce, M.I. (2007), "Appraisal of long-term effects of fly ash and silica fume on compressive strength of concrete by neural networks", *Constr. Build. Mater*., **21**(2), 384-394.

Patel, R., Hossain, K.M.A., Shehata, M., Bouzoubaâ, N. and Lachemi, M. (2004), "Development of statistical models for mixture design of high-volume fly ash self-consolidating concrete", *ACI. Mater. J*., **101**(4), 294-302.

Pathak, N. and Siddique, R. (2012), "Properties of self-compacting-concrete containing fly ash subjected to elevated temperatures", *Constr. Build. Mater*., **30**, 274-280.

Pedrycz, W., Succi, G., Sillitti, A. and Iljazi, J. (2015), "Data description: A general framework of information granules", *Knowledge-Based Syst.*, **80**, 98-108.

Peizhuang, W. (1983), "Pattern recognition with fuzzy objective function algorithms (James C. Bezdek)", *SIAM Rev*., **25**(3), 442-442.

Persson, B. (2001), "A comparison between mechanical propel-ties of self-compacting concrete and the corresponding properties of normal concrete", *Cement Concrete Res*., **31**(2), 193-198.

Pham, A.D., Hoang, N.D. and Nguyen, Q.T. (2016), "Predicting compressive strength of high-performance concrete using Metaheuristic-Optimized least squares support vector regression", *J. Comput. Civil Eng*., **30**(3), 1-4.

Phan, T.H., Chaouche, M. and Moranville, M. (2006), "Influence of organic admixtures on the rheological behaviour of cement pastes", *Cement Concrete Res*., **36**(10), 1807-1813.

Pofale, A.D. and Deo, S.V. (2010), "Comparative long term study of concrete mix design procedure for fine aggregate replacement with fly ash by minimum voids method and maximum density method", *KSCE. J. Civil Eng*., **14**(5), 759-764.

Rebouh, R., Boukhatem, B., Ghrici, M. and Tagnit-Hamou, A.

(2017), “A practical hybrid NNGA system for predicting the compressive strength of concrete containing natural pozzolan using an evolutionary structure”, *Constr. Build. Mater*., **149**, 778-789.

Roh, S.B., Oh, S.K. and Pedrycz, W. (2011), “Design of fuzzy radial basis function-based polynomial neural networks”, *Fuzzy Set. Syst*., **185**(1), 15-37.

Saha, P., Prasad, M.L.V. and RathishKumar, P. (2017), “Predicting strength of SCC using artificial neural network and multivariable regression analysis”, *Comput. Concrete*., **20**(1), 31-38.

Şahmaran, M., Christianto, H.A. and Yaman, I.O. (2006), “The effect of chemical admixtures and mineral additives on the properties of self-compacting mortars”, *Cement Concrete Compos*., **28**(5), 432-440.

Şahmaran, M., Lachemi, M., Erdem, T.K. and Yücel, H.E. (2011), “Use of spent foundry sand and fly ash for the development of green self-consolidating concrete”, *Mater. Struct*., **44**(7), 1193-1204.

Sánchez, L., Couso, I. and Casillas, J. (2009), “Genetic learning of fuzzy rules based on low quality data”, *Fuzzy Set. Syst*., **160**(17), 2524-2552.

Sandhir, R.P., Muhuri, S. and Nayak, T.K. (2012), “Dynamic fuzzy c-means (dFCM) clustering and its application to calorimetric data reconstruction in high-energy physics”, *Nucl. Instruments Methods Phys. Res. Sect. A Accel. Spectrometers, Detect. Assoc. Equip*., DOI: 10.1016/j.nima.2012.04.023.

Saridemir, M. (2009a), “Predicting the compressive strength of mortars containing metakaolin by artificial neural networks and fuzzy logic”, *Adv. Eng. Softw.*, **40**(9), 920-927.

Saridemir, M. (2009b), “Prediction of compressive strength of concretes containing metakaolin and silica fume by artificial neural networks”, *Adv. Eng. Softw*., **40**(5), 350-355.

Sarıdemir, M. (2014), “Effect of specimen size and shape on compressive strength of concrete containing fly ash: Application of genetic programming for design”, *Mater. Des*., **56**, 297-304.

Sarıdemir, M., Topçu, İ.B., Özcan, F. and Severcan, M.H. (2009), “Prediction of long-term effects of GGBFS on compressive strength of concrete by artificial neural networks and fuzzy logic”, *Constr. Build. Mater*., **23**(3), 1279-1286.

Shaikh, F.U.A. and Supit, S.W.M. (2014), “Mechanical and durability properties of high volume fly ash (HVFA) concrete containing calcium carbonate ($CaCO_3$) nanoparticles”, *Constr. Build. Mater*., **70**, 309-321.

Shaikh, F.U.A. and Supit, S.W.M. (2015), “Compressive strength and durability properties of high volume fly ash (HVFA) concretes containing ultrafine fly ash (UFFA)”, *Constr. Build. Mater*., **82**, 192-205.

Siad, H., Mesbah, H.A., Mouli, M., Escadeillas, G. and Khelafi, H. (2014), “Influence of mineral admixtures on the permeation properties of self-compacting concrete at different ages”, *Arab. J. Sci. Eng*., **39**(5), 3641-3649.

Siddique, R. (2011), “Properties of self-compacting concrete containing class F fly ash”, *Mater Des*., **32**(3), 1501-1507.

Siddique, R., Aggarwal, P. and Aggarwal, Y. (2011), “Prediction of compressive strength of self-compacting concrete containing bottom ash using artificial neural networks”, *Adv. Eng. Softw*., **42**(10), 780-786.

Siddique, R., Aggarwal, P. and Aggarwal, Y. (2012), “Influence of water/powder ratio on strength properties of self-compacting concrete containing coal fly ash and bottom ash”, *Constr. Build. Mater*., **29**, 73-81.

Simon, D. (2008), “Biogeography-Based Optimization”, *IEEE Tran. Evol. Comput*., **12**(6), 702-713.

Słoński, M. (2010), “A comparison of model selection methods for compressive strength prediction of high-performance concrete using neural networks”, *Comput. Struct*., **88**(21-22), 1248-1253.

Sonebi, M. (2004), “Medium strength self-compacting concrete containing fly ash: Modelling using factorial experimental plans”, *Cement Concrete Res*., **34**(7), 1199-1208.

Sonebi, M. and Cevik, A. (2009a), “Genetic programming based formulation for fresh and hardened properties of self-compacting concrete containing pulverised fuel ash”, *Constr. Build. Mater*., **23**(7), 2614-2622.

Sonebi, M. and Cevik, A. (2009b), “Prediction of fresh and hardened properties of self-consolidating concrete using neurofuzzy approach”, *J. Mater. Civil Eng*., **21**(11), 672-679.

Sukumar, B., Nagamani, K. and Srinivasa Raghavan, R. (2008), “Evaluation of strength at early ages of self-compacting concrete with high volume fly ash”, *Constr. Build. Mater*., **22**(7), 1394-1401.

Tayfur, G., Erdem, T.K. and Önder, K. (2014), “Strength prediction of high-strength concrete by fuzzy logic and artificial neural networks”, *J. Mater. Civil Eng*., **26**(11), 04014079.

Topçu, İ.B. and Sarıdemir, M. (2008), “Prediction of compressive strength of concrete containing fly ash using artificial neural networks and fuzzy logic”, *Comput. Mater. Sci*., **41**(3), 305-311.

Ulucan, Z.Ç., Türk, K. and Karataş, M. (2008), “Effect of mineral admixtures on the correlation between ultrasonic velocity and compressive strength for self-compacting concrete”, *Russ. J. Nondestruct. Test*., **44**(5), 367-374.

Utilisation, F. (2008), *2nd Annual International Summit*, New Dehli, India.

Uysal, M. and Sumer, M. (2011), “Performance of self-compacting concrete containing different mineral admixtures”, *Constr. Build. Mater*., **25**(11), 4112-4120.

Uysal, M. and Tanyildizi, H. (2011), “Predicting the core compressive strength of self-compacting concrete (SCC) mixtures with mineral additives using artificial neural network”, *Constr. Build. Mater*., **25**(11), 4105-4111.

Uysal, M. and Tanyildizi, H. (2012), “Estimation of compressive strength of self compacting concrete containing polypropylene fiber and mineral additives exposed to high temperature using artificial neural network”, *Constr. Build. Mater*., **27**(1), 404-414.

Valipour, M., Pargar, F., Shekarchi, M. and Khani, S. (2013), “Comparing a natural pozzolan, zeolite, to metakaolin and silica fume in terms of their effect on the durability characteristics of concrete: A laboratory study”, *Constr. Build. Mater*., **41**, 879-888.

Yang, Y.K., Sun, T.Y., Huo, C.L., Yu, Y.H., Liu, C.C. and Tsai, C.H. (2013), “A novel self-constructing Radial Basis Function Neural-Fuzzy System”, *Appl. Soft Comput. J*., **13**(5), 2390-2404.

Yu, J. and Duan, H. (2013), “Artificial Bee Colony approach to information granulation-based fuzzy radial basis function neural networks for image fusion”, *Opt. Int. J. Light Electron. Opt*., **127**(17), 3103-3111.

Zhao, H., Sun, W., Wu, X. and Gao, B. (2015), “The properties of the self-compacting concrete with fly ash and ground granulated blast furnace slag mineral admixtures”, *J. Clean. Prod*., **95**, 66-74.

Zheng, Y.J., Ling, H.F. and Xue, J.Y. (2014), “Ecogeography-based optimization: Enhancing biogeography-based optimization with ecogeographic barriers and differentiations”, *Comput. Oper. Res*., **50**, 115-127.

Zhu, W. and Bartos, P.J.M. (2003), “Permeation properties of self-compacting concrete”, *Cement Concrete Res*., **33**(6), 921-926.

Zhu, W., Gibbs, J.C. and Bartos, P.J.M. (2001), “Uniformity of in situ properties of self-compacting concrete in full-scale structural elements”, *Cement Concrete Compos*., **23**(1), 57-64.

HK

Appendix

Data used for training phase.

Row	Reference	*C* (Kg/m3)	*W* (Kg/m3)	*FA* (Kg/m3)	*CAgg* (Kg/m3)	*FAgg* (Kg/m3)	*SP* (%)	*A* (Days)	f_c (MPa)	Proposed model (MPa)
1	(Sonebi 2004)	290.00	175.50	100.00	837.00	913.00	0.80	7	32.30	32.21
2		250.00	281.05	261.00	837.00	478.00	0.50	7	9.60	7.30
3		210.00	193.50	220.00	837.00	768.00	0.80	7	15.50	15.37
4		290.00	253.50	100.00	837.00	709.00	0.20	7	12.80	10.14
5		290.00	229.50	220.00	837.00	625.00	0.20	7	11.50	16.69
6		250.00	225.50	160.00	837.00	742.00	0.50	7	16.90	18.01
7		250.00	225.50	160.00	837.00	739.00	0.00	7	15.50	13.36
8		317.00	262.35	160.00	837.00	594.00	0.50	7	17.00	17.12
9		210.00	279.50	220.00	837.00	562.00	0.20	7	6.20	6.36
10		250.00	225.50	160.00	837.00	742.00	0.50	7	14.70	18.01
11		250.00	155.80	160.00	837.00	919.00	0.50	7	23.90	20.48
12		183.00	188.65	160.00	837.00	981.00	0.50	7	12.00	10.22
13		210.00	201.50	100.00	837.00	910.00	0.80	28	19.10	22.11
14		250.00	225.50	160.00	837.00	742.00	0.50	28	24.10	25.04
15		210.00	193.50	220.00	837.00	768.00	0.80	28	26.70	28.40
16		290.00	229.50	220.00	837.00	625.00	0.20	28	32.90	28.58
17		210.00	279.50	220.00	837.00	562.00	0.20	28	10.20	12.30
18		250.00	225.50	160.00	837.00	742.00	0.50	28	25.30	25.04
19		250.00	155.80	160.00	837.00	919.00	0.50	28	36.30	40.14
20		250.00	225.50	160.00	837.00	746.00	1.00	28	26.70	25.26
21		250.00	295.20	160.00	837.00	566.00	0.50	28	11.00	11.71
22		183.00	188.65	160.00	837.00	981.00	0.50	28	22.10	23.89
23		290.00	175.50	100.00	837.00	913.00	0.80	90	55.90	55.34
24		250.00	281.05	261.00	837.00	478.00	0.50	90	29.50	31.76
25		210.00	201.50	100.00	837.00	910.00	0.80	90	28.00	24.69
26		250.00	225.50	160.00	837.00	742.00	0.50	90	41.50	40.05
27		210.00	193.50	220.00	837.00	768.00	0.80	90	45.60	43.10
28		290.00	253.50	100.00	837.00	709.00	0.20	90	35.70	38.60
29		250.00	225.50	160.00	837.00	742.00	0.50	90	42.80	40.05
30		250.00	225.50	160.00	837.00	739.00	0.00	90	42.00	42.61
31		317.00	262.35	160.00	837.00	594.00	0.50	90	29.10	28.99
32		210.00	279.50	220.00	837.00	562.00	0.20	90	19.70	17.53
33		250.00	225.50	160.00	837.00	742.00	0.50	90	39.20	40.05
34		250.00	225.50	160.00	837.00	746.00	1.00	90	40.30	41.18
35		250.00	295.20	160.00	837.00	566.00	0.50	90	17.20	16.47
36	(Patel *et al.* 2004)	220.00	156.00	180.00	900.00	916.00	0.35	1	12.50	12.68
37		248.00	176.00	203.00	900.00	808.00	0.35	1	12.00	17.13
38		237.00	157.00	133.00	900.00	960.00	0.50	1	16.00	17.24
39		280.00	156.00	120.00	900.00	946.00	0.35	1	16.00	15.03
40		220.00	156.00	180.00	900.00	916.00	0.35	1	12.00	12.68
41		198.00	153.00	232.00	900.00	872.00	0.50	1	13.00	13.93
42		170.00	157.00	200.00	900.00	928.00	0.50	1	5.00	2.85
43		220.00	156.00	180.00	900.00	916.00	0.35	28	49.00	47.17
44		160.00	156.00	240.00	900.00	886.00	0.35	28	44.00	44.10
45		198.00	153.00	232.00	900.00	874.00	0.20	28	46.00	45.98
46		248.00	176.00	203.00	900.00	808.00	0.35	28	50.00	45.13
47		220.00	156.00	180.00	900.00	916.00	0.35	28	49.00	47.17
48		237.00	157.00	133.00	900.00	960.00	0.50	28	46.00	45.92
49		280.00	156.00	120.00	900.00	946.00	0.35	28	45.00	44.82
50		170.00	157.00	200.00	900.00	930.00	0.20	28	31.00	31.48
51		220.00	156.00	180.00	900.00	916.00	0.35	28	45.00	47.17
52		170.00	157.00	200.00	900.00	928.00	0.50	28	33.00	34.47

Data used for training phase.

Row	Reference	*C* (Kg/m3)	*W* (Kg/m3)	*FA* (Kg/m3)	*CAgg* (Kg/m3)	*FAgg* (Kg/m3)	*SP* (%)	*A* (Days)	f_c (MPa)	Proposed model (MPa)
53	(Bouzoubaâ and Lechami 2001)	247.00	185.40	165.00	846.00	845.00	0.31	1	8.70	11.99
54		238.00	158.80	159.00	844.00	844.00	0.77	1	10.70	14.01
55		207.00	186.30	207.00	843.00	845.00	0.10	1	6.10	6.46
56		200.00	160.00	200.00	843.00	842.00	0.45	1	7.00	9.24
57		197.00	137.90	197.00	856.00	856.00	0.75	1	7.80	11.39
58		169.00	190.35	254.00	853.00	853.00	0.00	1	5.20	5.54
59		163.00	163.20	245.00	851.00	851.00	0.51	1	4.90	5.20
60		61.00	140.70	241.00	864.00	866.00	1.04	1	7.30	13.68
61		238.00	158.80	159.00	844.00	844.00	0.77	7	25.80	20.60
62		232.00	135.45	155.00	847.00	846.00	1.03	7	31.30	30.24
63		207.00	186.30	207.00	843.00	845.00	0.10	7	17.40	14.56
64		200.00	160.00	200.00	843.00	842.00	0.45	7	19.30	17.19
65		197.00	137.90	197.00	856.00	856.00	0.75	7	22.90	18.63
66		163.00	163.20	245.00	851.00	851.00	0.51	7	14.70	12.95
67		247.00	185.40	165.00	846.00	845.00	0.31	28	34.60	32.85
68		238.00	158.80	159.00	844.00	844.00	0.77	28	37.80	40.26
69		232.00	135.45	155.00	847.00	846.00	1.03	28	48.30	49.58
70		200.00	160.00	200.00	843.00	842.00	0.45	28	34.90	35.14
71		169.00	190.35	254.00	853.00	853.00	0.00	28	30.20	30.94
72		163.00	163.20	245.00	851.00	851.00	0.51	28	26.20	28.10
73		61.00	140.70	241.00	864.00	866.00	1.04	28	35.80	29.47
74	(Bui *et al*. 2002)	350.00	174.00	186.00	851.00	786.00	0.45	1	18.30	32.23
75		380.00	200.00	192.00	621.00	931.00	0.40	1	23.20	23.09
76		380.00	184.00	145.00	854.00	788.00	0.42	7	53.20	53.86
77		350.00	174.00	186.00	851.00	786.00	0.45	7	51.10	43.17
78		380.00	184.00	145.00	854.00	788.00	0.42	28	73.50	72.42
79		350.00	174.00	186.00	851.00	786.00	0.45	28	70.40	65.98
80		380.00	200.00	192.00	621.00	931.00	0.40	28	67.80	68.12
81	(Şahmaran *et al.* 2011)	315.00	180.00	135.00	831.00	831.00	0.40	7	32.07	25.27
82		135.00	180.00	315.00	805.00	805.00	0.26	7	17.47	20.44
83		315.00	180.00	135.00	831.00	831.00	0.40	28	38.28	44.33
84		225.00	180.00	225.00	818.00	818.00	0.35	28	42.67	41.34
85		135.00	180.00	315.00	805.00	805.00	0.26	28	36.09	33.62
86		225.00	180.00	225.00	818.00	818.00	0.35	90	45.93	48.83
87		135.00	180.00	315.00	805.00	805.00	0.26	90	39.88	39.48
88	(Sonebi and Cevik 2009b)	270.00	247.50	180.00	837.00	647.00	0.60	7	14.60	13.05
89		280.00	258.50	190.00	837.00	599.00	0.70	7	14.70	16.06
90		240.00	202.80	150.00	837.00	831.00	0.60	7	19.00	20.98
91		270.00	247.50	180.00	837.00	647.00	0.60	28	24.50	24.40
92		230.00	192.40	140.00	837.00	864.00	0.80	28	32.10	30.29
93		240.00	202.80	150.00	837.00	831.00	0.60	28	30.90	28.39
94		270.00	247.50	180.00	837.00	647.00	0.60	90	37.20	38.67
95		280.00	258.50	190.00	837.00	599.00	0.70	90	36.50	35.58
96		260.00	227.90	170.00	837.00	717.00	0.70	90	38.20	38.25
97		230.00	192.40	140.00	837.00	864.00	0.80	90	43.50	45.18
98		240.00	202.80	150.00	837.00	831.00	0.60	90	44.20	45.70
99	(Chabib and Syed 2012)	180.00	166.50	270.00	850.00	850.00	0.20	90	32.32	31.12
100	(Mohamed 2011)	405.00	189.00	45.00	612.00	1109.00	4.60	7	12.77	13.45
101		382.50	189.00	67.50	612.00	1109.00	4.60	7	13.10	12.48
102		360.00	189.00	90.00	612.00	1109.00	4.60	7	15.00	16.99
103		315.00	189.00	135.00	612.00	1109.00	4.60	7	25.33	20.70
104		292.50	189.00	157.50	612.00	1109.00	4.60	7	18.44	19.08
105		270.00	189.00	180.00	612.00	1109.00	4.60	7	17.56	19.18
106		225.00	189.00	225.00	612.00	1109.00	4.60	7	12.09	13.68

Data used for training phase.

Row	Reference	*C* (Kg/m3)	*W* (Kg/m3)	*FA* (Kg/m3)	*CAgg* (Kg/m3)	*FAgg* (Kg/m3)	*SP* (%)	*A* (Days)	f_c (MPa)	Proposed model (MPa)
107		467.50	231.00	82.50	612.00	909.00	3.81	7	16.71	14.73
108		440.00	231.00	110.00	612.00	909.00	3.81	7	17.57	17.41
109		412.50	231.00	137.50	612.00	909.00	3.81	7	18.68	21.74
110		385.00	231.00	165.00	612.00	909.00	3.81	7	26.71	24.38
111		330.00	231.00	220.00	612.00	909.00	3.81	7	16.96	17.44
112		275.00	231.00	275.00	612.00	909.00	3.81	7	12.32	12.33
113		405.00	189.00	45.00	612.00	1109.00	4.60	28	15.99	14.68
114		382.50	189.00	67.50	612.00	1109.00	4.60	28	16.56	16.21
115		360.00	189.00	90.00	612.00	1109.00	4.60	28	21.66	23.19
116		315.00	189.00	135.00	612.00	1109.00	4.60	28	28.95	30.02
117		225.00	189.00	225.00	612.00	1109.00	4.60	28	19.21	17.13
118		495.00	231.00	55.00	612.00	909.00	3.81	28	17.20	19.36
119		467.50	231.00	82.50	612.00	909.00	3.81	28	18.30	17.59
120		440.00	231.00	110.00	612.00	909.00	3.81	28	23.27	21.73
121		412.50	231.00	137.50	612.00	909.00	3.81	28	25.12	27.18
122		385.00	231.00	165.00	612.00	909.00	3.81	28	30.01	29.36
123		330.00	231.00	220.00	612.00	909.00	3.81	28	19.93	19.86
124	(Siad *et al.* 2014)	260.00	215.00	260.00	775.00	757.00	0.77	28	30.90	30.19
125		450.00	188.00	70.00	844.00	825.00	2.34	28	70.80	71.87
126		260.00	215.00	260.00	775.00	757.00	0.77	90	39.30	40.19
127		350.00	214.00	170.00	792.00	774.00	0.81	90	61.10	60.69
128		450.00	188.00	70.00	844.00	825.00	2.34	90	78.60	76.97
129		260.00	215.00	260.00	775.00	757.00	0.77	365	54.90	55.41
130		350.00	214.00	170.00	792.00	774.00	0.81	365	74.10	73.37
131		450.00	188.00	70.00	844.00	825.00	2.34	365	90.60	91.04
132	(da Silva *et al.* 2015)	290.00	180.00	318.00	700.00	741.00	0.66	7	34.40	33.71
133		218.00	178.00	373.00	700.00	743.00	0.51	7	21.60	22.12
134		503.00	183.00	158.00	700.00	735.00	0.76	28	68.40	67.42
135		218.00	178.00	373.00	700.00	743.00	0.51	28	35.30	35.98
136		503.00	183.00	158.00	700.00	735.00	0.76	90	71.70	73.70
137		290.00	180.00	318.00	700.00	741.00	0.66	90	62.50	63.13
138		218.00	178.00	373.00	700.00	743.00	0.51	90	48.90	47.31
139		503.00	183.00	158.00	700.00	735.00	0.76	182	69.50	68.10
140		290.00	180.00	318.00	700.00	741.00	0.66	182	59.90	60.75
141	(Khatib 2008)	400.00	180.00	20.00	876.00	845.00	0.70	1	16.99	24.17
142		300.00	180.00	40.00	876.00	813.00	0.70	1	14.99	24.65
143		200.00	180.00	60.00	876.00	782.00	0.70	1	4.00	9.89
144		400.00	180.00	20.00	876.00	845.00	0.70	7	39.60	30.37
145		300.00	180.00	40.00	876.00	813.00	0.70	7	39.15	32.55
146		200.00	180.00	60.00	876.00	782.00	0.70	7	19.59	12.27
147		100.00	180.00	80.00	876.00	751.00	0.70	7	5.19	3.29
148		400.00	180.00	20.00	876.00	845.00	0.70	28	50.19	48.52
149		300.00	180.00	40.00	876.00	813.00	0.70	28	52.99	52.02
150		200.00	180.00	60.00	876.00	782.00	0.70	28	30.00	29.07
151		100.00	180.00	80.00	876.00	751.00	0.70	28	9.59	8.85
152		400.00	180.00	20.00	876.00	845.00	0.70	56	56.80	61.26
153		300.00	180.00	40.00	876.00	813.00	0.70	56	63.79	62.25
154		200.00	180.00	60.00	876.00	782.00	0.70	56	36.40	37.90
155		100.00	180.00	80.00	876.00	751.00	0.70	56	10.80	13.77
156	(Liu 2010)	437.00	176.00	80.00	924.00	743.00	0.90	7	47.79	46.70
157		333.00	173.00	162.00	924.00	743.00	0.75	7	38.97	35.29
158		225.00	170.00	247.00	924.00	743.00	0.68	7	22.05	19.88
159		115.00	167.00	336.00	924.00	743.00	0.65	7	7.56	3.21
160		437.00	176.00	80.00	924.00	743.00	0.90	28	62.73	62.18

Data used for training phase.

Row	Reference	*C* (Kg/m3)	*W* (Kg/m3)	*FA* (Kg/m3)	*CAgg* (Kg/m3)	*FAgg* (Kg/m3)	*SP* (%)	*A* (Days)	f_c (MPa)	Proposed model (MPa)
161		333.00	173.00	162.00	924.00	743.00	0.75	28	52.65	56.27
162		225.00	170.00	247.00	924.00	743.00	0.68	28	33.48	34.14
163		115.00	167.00	336.00	924.00	743.00	0.65	28	14.40	15.58
164		437.00	176.00	80.00	924.00	743.00	0.90	90	70.20	72.16
165		333.00	173.00	162.00	924.00	743.00	0.75	90	56.70	55.68
166		225.00	170.00	247.00	924.00	743.00	0.68	90	44.37	46.56
167		115.00	167.00	336.00	924.00	743.00	0.65	90	23.49	27.23
168		437.00	176.00	80.00	924.00	743.00	0.90	180	74.88	72.84
169		333.00	173.00	162.00	924.00	743.00	0.75	180	61.20	62.61
170		225.00	170.00	247.00	924.00	743.00	0.68	180	50.76	48.01
171	(Zhao *et al.* 2015)	322.00	161.00	138.00	1058.20	693.81	0.24	3	29.49	36.17
172		276.00	161.00	184.00	1058.20	693.81	0.24	3	23.85	30.11
173		368.00	161.00	92.00	1058.20	693.81	0.24	7	47.24	44.92
174		322.00	161.00	138.00	1058.20	693.81	0.24	7	41.18	37.10
175		276.00	161.00	184.00	1058.20	693.81	0.24	7	39.38	31.72
176		368.00	161.00	92.00	1058.20	693.81	0.24	90	67.15	69.94
177		322.00	161.00	138.00	1058.20	693.81	0.24	90	65.35	62.16
178		276.00	161.00	184.00	1058.20	693.81	0.24	90	64.49	66.45
179	(Pathak and Siddique 2012)	300.00	200.00	200.00	860.00	845.00	1.80	28	23.49	23.05
180		350.00	190.00	150.00	876.00	830.00	1.82	90	35.60	35.92
181		250.00	210.00	250.00	856.00	856.00	1.72	90	27.29	27.70
182	(Gesoğlu and Özbay 2007)	440.00	176.00	110.00	917.00	714.00	1.35	28	62.82	62.83
183		330.00	176.00	220.00	899.00	700.00	1.35	28	54.81	54.76
184		220.00	176.00	330.00	881.00	686.00	1.21	28	42.75	44.19
185	(Pofale and Deo 2010)	386.00	193.00	161.00	1190.00	434.00	0.00	7	21.33	18.66
186		386.00	193.00	72.00	1190.00	523.00	0.00	7	19.71	22.06
187		386.00	193.00	161.00	1190.00	434.00	1.93	7	23.49	21.97
188		386.00	193.00	72.00	1190.00	523.00	1.93	7	22.05	25.04
189		386.00	193.00	161.00	1190.00	434.00	0.00	28	30.51	33.03
190		386.00	193.00	72.00	1190.00	523.00	0.00	28	28.17	25.93
191		386.00	193.00	161.00	1190.00	434.00	1.93	28	33.21	34.82
192		386.00	193.00	72.00	1190.00	523.00	1.93	28	31.77	28.68
193	(Ulucan *et al.* 2008)	375.00	195.00	125.00	735.00	910.00	1.35	3	24.89	24.53
194		350.00	190.00	150.00	735.00	910.00	1.35	3	21.70	24.61
195		325.00	190.00	175.00	735.00	910.00	1.35	3	20.12	20.47
196		300.00	190.00	200.00	735.00	910.00	1.35	3	18.08	21.73
197		375.00	195.00	125.00	735.00	910.00	1.35	7	27.33	27.08
198		350.00	190.00	150.00	735.00	910.00	1.35	7	30.21	27.53
199		325.00	190.00	175.00	735.00	910.00	1.35	7	26.81	24.22
200		300.00	190.00	200.00	735.00	910.00	1.35	7	25.15	24.40
201		375.00	195.00	125.00	735.00	910.00	1.35	28	44.45	43.40
202		350.00	190.00	150.00	735.00	910.00	1.35	28	40.60	42.57
203		300.00	190.00	200.00	735.00	910.00	1.35	28	40.73	39.83
204		375.00	195.00	125.00	735.00	910.00	1.35	130	48.20	50.34
205		350.00	190.00	150.00	735.00	910.00	1.35	130	49.72	50.59
206		325.00	190.00	175.00	735.00	910.00	1.35	130	52.30	51.33
207		300.00	190.00	200.00	735.00	910.00	1.35	130	53.14	51.40
208	(Bingöl and Tohumcu 2013)	225.00	175.00	275.00	652.00	908.00	1.50	3	36.21	32.87
209		375.00	175.00	125.00	673.00	938.00	1.50	7	53.91	53.23
210		300.00	175.00	200.00	663.00	923.00	1.50	7	44.08	44.86
211		225.00	175.00	275.00	652.00	908.00	1.50	7	36.77	34.45
212		375.00	175.00	125.00	673.00	938.00	1.50	28	55.20	55.50
213		300.00	175.00	200.00	663.00	923.00	1.50	28	49.15	48.43
214		225.00	175.00	275.00	652.00	908.00	1.50	28	37.76	43.17

Data used for training phase.

Row	Reference	*C* (Kg/m3)	*W* (Kg/m3)	*FA* (Kg/m3)	*CAgg* (Kg/m3)	*FAgg* (Kg/m3)	*SP* (%)	*A* (Days)	f_c (MPa)	Proposed model (MPa)
215	(Siddique *et al.* 2012)	465.00	225.50	85.00	590.00	910.00	1.95	28	31.80	30.61
216		440.00	225.50	110.00	590.00	910.00	2.00	28	29.98	31.56
217		415.00	231.00	135.00	590.00	910.00	1.80	28	28.35	27.87
218		385.00	236.50	165.00	590.00	910.00	1.80	28	27.63	26.26
219		355.00	242.00	195.00	590.00	910.00	1.80	28	26.74	28.74
220		415.00	231.00	135.00	590.00	910.00	1.80	90	39.48	41.64
221		385.00	236.50	165.00	590.00	910.00	1.80	90	37.86	35.48
222		355.00	242.00	195.00	590.00	910.00	1.80	90	36.76	36.25
223		465.00	225.50	85.00	590.00	910.00	1.95	365	55.26	52.95
224		415.00	231.00	135.00	590.00	910.00	1.80	365	41.91	45.23
225		385.00	236.50	165.00	590.00	910.00	1.80	365	40.41	40.82
226		355.00	242.00	195.00	590.00	910.00	1.80	365	39.33	37.92
227	(Güneyisi *et al.* 2015)	427.50	188.10	142.50	812.10	812.10	0.50	28	45.00	45.03
228		285.50	188.10	285.00	788.70	788.70	0.40	28	52.88	52.59
229		142.50	188.10	427.50	765.30	765.40	0.30	28	58.82	58.73
230	(Güneyisi *et al.* 2010)	440.00	176.00	110.00	917.00	714.00	1.35	28	62.82	62.83
231		330.00	176.00	220.00	899.00	700.00	1.35	28	54.81	54.76
232		220.00	176.00	330.00	881.00	686.00	1.21	28	42.75	44.19
233		360.00	198.00	90.00	855.00	813.00	0.71	28	46.89	46.36
234		270.00	198.00	180.00	842.00	801.00	0.66	28	40.23	38.69
235		180.00	198.00	270.00	829.00	778.00	0.67	28	27.27	26.54
236		440.00	176.00	110.00	917.00	714.00	1.35	90	75.96	76.76
237		220.00	176.00	330.00	881.00	686.00	1.21	90	58.32	55.24
238		270.00	198.00	180.00	842.00	801.00	0.66	90	54.27	55.26
239		180.00	198.00	270.00	829.00	778.00	0.67	90	38.25	38.59
240	(Sukumar *et al.* 2008)	250.00	178.50	275.00	772.00	842.00	0.40	1	7.33	13.85
241		333.00	180.84	215.00	766.00	835.00	0.40	1	9.29	15.31
242		417.00	182.40	153.00	759.00	828.00	0.50	1	11.48	19.94
243		500.00	192.32	101.00	753.00	820.00	0.60	1	13.15	26.07
244		583.00	196.23	50.00	745.00	813.00	0.70	1	14.59	25.18
245		250.00	178.50	275.00	772.00	842.00	0.40	3	16.31	17.11
246		333.00	180.84	215.00	766.00	835.00	0.40	3	20.92	18.92
247		417.00	182.40	153.00	759.00	828.00	0.50	3	25.45	25.61
248		500.00	192.32	101.00	753.00	820.00	0.60	3	28.96	29.52
249		250.00	178.50	275.00	772.00	842.00	0.40	7	24.84	19.96
250		333.00	180.84	215.00	766.00	835.00	0.40	7	31.73	23.42
251		417.00	182.40	153.00	759.00	828.00	0.50	7	39.19	30.59
252		500.00	192.32	101.00	753.00	820.00	0.60	7	44.83	37.08
253		583.00	196.23	50.00	745.00	813.00	0.70	7	50.33	38.99
254		250.00	178.50	275.00	772.00	842.00	0.40	14	31.42	26.38
255		333.00	180.84	215.00	766.00	835.00	0.40	14	39.76	35.47
256		500.00	192.32	101.00	753.00	820.00	0.60	14	56.21	48.15
257		583.00	196.23	50.00	745.00	813.00	0.70	14	63.61	55.12
258		250.00	178.50	275.00	772.00	842.00	0.40	28	35.66	39.09
259		333.00	180.84	215.00	766.00	835.00	0.40	28	45.22	52.42
260		500.00	192.32	101.00	753.00	820.00	0.60	28	63.84	66.43
261		583.00	196.23	50.00	745.00	813.00	0.70	28	73.13	82.56
262	(Leung *et al.* 2016)	540.00	235.60	80.00	720.00	780.00	0.51	28	54.90	54.83
263		496.00	235.60	124.00	720.00	780.00	0.68	28	48.94	49.11
264		434.00	235.60	186.00	720.00	780.00	0.68	28	47.34	47.16
265		310.00	235.60	310.00	720.00	780.00	0.57	28	34.31	34.27
266	(Le and Ludwig 2016)	347.00	151.00	232.00	968.00	790.00	2.50	3	52.38	58.81
267		347.00	151.00	232.00	968.00	790.00	2.50	7	67.77	63.77
268		481.00	156.00	120.00	968.00	790.00	2.00	28	98.91	98.74
269		347.00	151.00	232.00	968.00	790.00	2.50	28	98.46	90.09
270		347.00	151.00	232.00	968.00	790.00	2.50	56	104.85	111.00

Data used for testing phase

Row	Reference	*C* (Kg/m^3)	*W* (Kg/m^3)	*FA* (Kg/m^3)	*CAgg* (Kg/m^3)	*FAgg* (Kg/m^3)	*SP* (%)	A (Days)	f_c (MPa)	Proposed model (MPa)
1	(Sonebi 2004)	210.00	201.50	100.00	837.00	910.00	0.80	7	11.10	12.08
2		250.00	225.50	160.00	837.00	742.00	0.50	7	13.90	17.86
3		250.00	225.50	160.00	837.00	746.00	1.00	7	15.80	17.38
4		250.00	295.20	160.00	837.00	566.00	0.50	7	6.20	8.65
5		290.00	175.50	100.00	837.00	913.00	0.80	28	42.70	47.48
6		250.00	281.05	261.00	837.00	478.00	0.50	28	17.00	16.09
7		290.00	253.50	100.00	837.00	709.00	0.20	28	26.60	19.00
8		250.00	225.50	160.00	837.00	742.00	0.50	28	28.50	25.06
9		250.00	225.50	160.00	837.00	739.00	0.00	28	27.30	23.65
10		317.00	262.35	160.00	837.00	594.00	0.50	28	29.10	20.53
11		290.00	229.50	220.00	837.00	625.00	0.20	90	44.90	47.66
12		250.00	155.80	160.00	837.00	919.00	0.50	90	48.30	51.17
13		183.00	188.65	160.00	837.00	981.00	0.50	90	34.20	27.24
14	(Patel *et al.* 2004)	160.00	156.00	240.00	900.00	886.00	0.35	1	7.00	11.82
15		198.00	153.00	232.00	900.00	874.00	0.20	1	9.00	12.54
16		220.00	156.00	180.00	900.00	916.00	0.35	1	13.00	12.68
17		170.00	157.00	200.00	900.00	930.00	0.20	1	6.00	2.94
18		220.00	156.00	180.00	900.00	916.00	0.35	1	13.00	12.68
19		220.00	156.00	180.00	900.00	916.00	0.35	28	47.00	47.17
20		198.00	153.00	232.00	900.00	872.00	0.50	28	52.00	54.01
21	(Bouzoubaâ and Lechami 2001)	232.00	135.45	155.00	847.00	846.00	1.03	1	16.60	22.93
22		247.00	185.40	165.00	846.00	845.00	0.31	7	21.20	21.32
23		169.00	190.35	254.00	853.00	853.00	0.00	7	15.60	12.70
24		61.00	140.70	241.00	864.00	866.00	1.04	7	20.60	16.07
25		207.00	186.30	207.00	843.00	845.00	0.10	28	33.20	30.08
26		197.00	137.90	197.00	856.00	856.00	0.75	28	38.90	40.53
27	(Bui *et al.* 2002)	380.00	184.00	145.00	854.00	788.00	0.42	1	26.90	40.50
28		380.00	200.00	192.00	621.00	931.00	0.40	7	45.70	32.98
29	(Şahmaran *et al.* 2011)	225.00	180.00	225.00	818.00	818.00	0.35	7	26.20	20.54
30		315.00	180.00	135.00	831.00	831.00	0.40	90	50.13	41.98
31	(Sonebi and Cevik 2009b)	260.00	227.90	170.00	837.00	717.00	0.70	7	16.70	14.95
32		230.00	192.40	140.00	837.00	864.00	0.80	7	19.30	16.61
33		280.00	258.50	190.00	837.00	599.00	0.70	28	24.00	20.56
34		260.00	227.90	170.00	837.00	717.00	0.70	28	27.80	20.45
35	(Chabib and Syed 2012)	180.00	166.50	270.00	850.00	850.00	0.20	1	5.00	0.54
36		180.00	166.50	270.00	850.00	850.00	0.20	7	14.72	7.13
37		180.00	166.50	270.00	850.00	850.00	0.20	28	23.65	19.67
38	(Mohamed 2011)	337.50	189.00	112.50	612.00	1109.00	4.60	7	19.66	20.57
39		495.00	231.00	55.00	612.00	909.00	3.81	7	16.51	17.70
40		337.50	189.00	112.50	612.00	1109.00	4.60	28	22.71	28.13
41		275.00	231.00	275.00	612.00	909.00	3.81	28	16.90	10.94
42	(Siad *et al.* 2014)	350.00	214.00	170.00	792.00	774.00	0.81	28	50.30	46.51
43	(da Silva *et al.* 2015)	503.00	183.00	158.00	700.00	735.00	0.76	7	58.80	47.18
44		290.00	180.00	318.00	700.00	741.00	0.66	28	54.00	50.75
45		218.00	178.00	373.00	700.00	743.00	0.51	182	49.60	51.65
46	(Liu 2010)	115.00	167.00	336.00	924.00	743.00	0.65	180	33.48	29.81
47	(Zhao *et al.* 2015)	368.00	161.00	92.00	1058.20	693.81	0.24	3	35.69	44.64
48		368.00	161.00	92.00	1058.20	693.81	0.24	28	58.46	46.55
49		322.00	161.00	138.00	1058.20	693.81	0.24	28	51.61	38.53
50		276.00	161.00	184.00	1058.20	693.81	0.24	28	49.49	41.20
51	(Pathak and Siddique 2012)	350.00	190.00	150.00	876.00	830.00	1.82	28	27.45	23.99
52		250.00	210.00	250.00	856.00	856.00	1.72	28	19.35	10.14
53		300.00	200.00	200.00	860.00	845.00	1.80	90	31.50	39.73
54	(Ulucan *et al.* 2008)	325.00	190.00	175.00	735.00	910.00	1.35	28	38.30	37.12
55	(Bingöl and Tohumcu 2013)	375.00	175.00	125.00	673.00	938.00	1.50	3	51.53	51.06
56		300.00	175.00	200.00	663.00	923.00	1.50	3	43.66	43.61
57	(Siddique *et al.* 2012)	465.00	225.50	85.00	590.00	910.00	1.95	90	53.14	52.93
58		440.00	225.50	110.00	590.00	910.00	2.00	90	47.52	47.74
59		440.00	225.50	110.00	590.00	910.00	2.00	365	49.14	44.04
60	(Güneyisi *et al.* 2010)	330.00	176.00	220.00	899.00	700.00	1.35	90	70.11	76.96
61		360.00	198.00	90.00	855.00	813.00	0.71	90	61.20	48.29
62	(Sukumar *et al.* 2008)	583.00	196.23	50.00	745.00	813.00	0.70	3	32.11	29.96
63		417.00	182.40	153.00	759.00	828.00	0.50	14	49.07	41.14
64		417.00	182.40	153.00	759.00	828.00	0.50	28	55.64	56.76
65	(Leung *et al.* 2016)	372.00	235.60	248.00	720.00	780.00	0.64	28	40.28	37.42
66	(Le and Ludwig 2016)	481.00	156.00	120.00	968.00	790.00	2.00	3	68.22	75.15
67		481.00	156.00	120.00	968.00	790.00	2.00	7	83.34	79.74
68		481.00	156.00	120.00	968.00	790.00	2.00	56	107.46	115.29